Available online at www.sciencedirect.com
ScienceDirect
Precambrian Research 155 (2007) 1–23
Precambrian Research
www.elsevier.com/locate/precamres

# Structural characterization of kerogen in 3.4 Ga Archaean cherts from the Pilbara Craton, Western Australia

Craig P. Marshall [a,b,*], Gordon D. Love [c,d,**], Colin E. Snape [e], Andrew C. Hill [f,b], Abigail C. Allwood [b], Malcolm R. Walter [b], Martin J. Van Kranendonk [g,b], Stephen A. Bowden [h], Sean P. Sylva [i], Roger E. Summons [c,b]

[a] *Vibrational Spectroscopy Facility, School of Chemistry, The University of Sydney, Sydney, NSW 2006, Australia*
[b] *Australian Centre for Astrobiology, Macquarie University Biotechnology Research Institute, Sydney, NSW 2109, Australia*
[c] *Department of Earth, Atmospheric and Planetary Sciences, MIT, Cambridge, MA 02139, USA*
[d] *Department of Earth Sciences, University of California Riverside, Riverside, CA 92521, USA*
[e] *School of Chemical, Environmental and Mining Engineering, University of Nottingham, University Park, Nottingham NG7 2RD, United Kingdom*
[f] *Centro de Astrobiología, Instituto Nacional de Técnica Aeroespacial (INTA-CSIC), Ctra de Ajalvir, km 4, 28850 Torrejón de Ardoz, Madrid, Spain*
[g] *Geological Survey of Western Australia, 100 Plain St, East Perth, Western Australia 6004, Australia*
[h] *Department of Geology and Petroleum Geology, University of Aberdeen, Aberdeen AB24 3EU, United Kingdom*
[i] *Department of Geology and Geophysiscs, Woods Hole Oceanographic Institution, Woods Hole, MA 02543, USA*

Received 17 May 2006; received in revised form 19 December 2006; accepted 21 December 2006

**Abstract**

Hydrogen-lean kerogen (atomic H/C < 0.46) isolated from the 3.4 Ga Strelley Pool Chert in the North Pole area, Pilbara Craton, Western Australia, were studied by vibrational spectroscopy (Fourier transform infrared (FTIR) spectroscopy and Raman spectroscopy), nuclear magnetic resonance spectroscopy (solid state $^{13}C$ NMR spectroscopy), catalytic hydropyrolysis followed by gas chromatography mass spectrometry (HyPy–GC–MS), and isotope ratio mass spectrometry (IRMS). The kerogen occurs in sedimentary rocks as clasts and clots deposited together with other detrital materials that are finely disseminated throughout a chert matrix. The bulk kerogen $\delta^{13}C$ values range from −28.3 to −35.8‰. Solid-state $^{13}C$ NMR spectroscopy and FTIR spectroscopy reveals that the kerogen is highly aromatic ($f_a$ varying from 0.90 to 0.92) and contains only minor aliphatic carbon or carbon-oxygenated (C–O) functionalities. The Raman carbon first-order spectra for the isolated kerogens are typical of spectra obtained from disordered $sp^2$ carbons with low 2-D ordering (biperiodic structure). The implications of the Raman results show low 2-D ordering throughout the carbonaceous network indicate the incorrect usage of the term *graphite* in the literature to describe the kerogen or carbonaceous material in the Warrawoona cherts. Hydropyrolysates contain aromatic compounds consisting of 1-ring to 7-ring polycyclic aromatic hydrocarbons which were covalently bound into the kerogen as well as alkanes (linear, branched and cyclic) which were most probably trapped in the microporous network of the kerogen. These PAHs have mainly C1- and C2-alkylation while $C_{3+}$-substitued aromatics are low in abundance and do not show a high degree of branched alkylation. For the first time we have shown a correlation between elemental analysis (H/C atomic ratios), Raman spectroscopic parameters ($I_{D1}/I_G$, $I_{D1}/(I_{D1}+I_G)$, and $L_a$), and the degree of alkylation of bound polyaromatic molecular constituents generated from HyPy for Archaean kerogens. Similarities in molecular

* Corresponding author at: Vibrational Spectroscopy Facility, School of Chemistry, The University of Sydney, Sydney, NSW 2006, Australia. Tel.: +61 2 9531 3994; fax: +61 2 9351 3329.
** Corresponding author at: Department of Earth Sciences, University of California Riverside, Riverside, CA 92521, USA.
*E-mail address:* c.marshall@chem.usyd.edu.au (C.P. Marshall).

0301-9268/$ – see front matter 
doi:10.1016/j.precamres.2006.12.014

profiles exist between HyPy products of Strelley Pool Chert kerogens and an oil-window-mature Mesoproterozoic kerogen from Roper Group (ca. 1.45 Ga), which is biogenic in origin, suggesting that the Strelley Pool Chert kerogens may also be derived from diagenesis and thermal processing of biogenic organic matter. A combination of Raman spectroscopy, for identifying the least metamorphosed kerogens, used together with HyPy for liberating trapped and bound molecular components of these kerogens, offers a powerful strategy for assessing the origins of Earth's oldest preserved organic matter.


*Keywords:* Archaean kerogens; Spectroscopy; HyPy–GC–MS; Pilbara craton; Strelley Pool chert

## 1. Introduction

Biological activity in the Early Archaean has been inferred from the occurrence of $^{13}C$ depleted organic matter (Mojzsis et al., 1996; Rosing, 1999; Schidlowski, 2001; Ueno et al., 2001a,b, 2002, 2004), microfossils (Awramik et al., 1983; Schopf, 1993; Schopf et al., 2002), stromatolites (Walter et al., 1980; Lowe, 1983; Hofmann et al., 1999; Van Kranendonk et al., 2003; Allwood et al., 2006a) and microstructures in volcanic glass (Furnes et al., 2004; Banerjee et al., 2006). However, the exact origin of 3.4–3.5 Ga microfossils and kerogens (Pilbara Craton, Western Australia) and 3.8 Ga graphite (Akilia, Greenland) is still a matter of debate (e.g., Brasier et al., 2002, 2005; Garcia Ruiz et al., 2003; Lepland et al., 2005; Lindsay et al., 2005). The Archaean Pilbara Craton, Western Australia, is an optimal location to search for preserved biosignatures from early Earth—it has a well-preserved, nearly continuous geological history from >3.5 through to 2.4 Ga, preserved in a relatively low metamorphic grade with low strain rocks. These sediments contain evidence of hydrothermal systems, stromatolites, and putative microfossils (Dunlop et al., 1978; Lowe, 1980; Walter et al., 1980; Awramik et al., 1983; Schopf, 1993; Hofmann et al., 1999; Van Kranendonk et al., 2002, 2003, 2005; Ueno et al., 2004; Van Kranendonk and Pirajno, 2004; Allwood et al., 2004, 2005, 2006a).

The occurrence of insoluble carbonaceous material, which has been incorrectly termed graphite (e.g., Brasier et al., 2002, 2005; Lindsay et al., 2005; McCollom and Seewald, 2006), associated with 'microfossil-like' structures in the ca. 3.46 Ga Warrawoona Group, Pilbara Craton, as revealed by Raman spectroscopy, was proposed as an additional line of evidence for a biogenic origin of the putative microfossils in a hydrothermal silica vein from the 3.46 Ga Apex chert (Schopf et al., 2002). Additionally, highly $^{13}C$-depleted $\delta^{13}C$ values from similar putative microfossils in hydrothermal silica veins in the ca. 3.49 Ga Dresser Formation (e.g., Ueno et al., 2004) was further taken as evidence for biogenicity. However, there is an ongoing debate about the precise origins of these putative microfossils because they occur in hydrothermal silica veins (Brasier et al., 2002; Van Kranendonk et al., 2005). Similar structures, in terms of morphology and Raman spectral features, can be formed through abiotic reactions such that these microstructures have also been interpreted as secondary artifacts formed under hydrothermal conditions (Brasier et al., 2002, 2005; Pasteris and Wopencka, 2002, 2003; Garcia Ruiz et al., 2003; Lindsay et al., 2005). Suggestions have also been made that the kerogens may have been introduced into the rocks by later fluid circulation (e.g., Buick, 1984). Therefore, significant interest has been stimulated in elucidating the macromolecular structure of the insoluble carbonaceous material in these cherts, in order to discriminate between a biological and non-biological origin (e.g., Sharp and De Gregorio, 2003; Derenne et al., 2004; Skrzypczak et al., 2004, 2005; Westall and Rouzaud, 2004; Marshall et al., 2004a,b; Rouzaud et al., 2005; Allwood et al., 2006b). One of the key issues in this debate is to establish whether the chemical structure of the macromolecular organic material is consistent with this being either thermally mature kerogen or crystalline graphite and whether any genuine and informative molecular or isotopic patterns can be detected from fragmentation products.

### 1.1. Previous studies of Archaean kerogens

Sharp and De Gregorio (2003) and De Gregorio et al. (2005) analyzed carbonaceous material preserved in the Apex chert of the Warrawoona Group using a combination of transmission electron microscopy (TEM), electron energy loss spectroscopy (EELS) and X-ray absorption near-edge spectroscopy (XANES). The carbonaceous material appeared amorphous under High Resolution Transmission Electron Microscopy (HRTEM), was mostly distributed along grain boundaries between quartz crystals, and was evaluated as "kerogen or amorphous carbon". The EELS spectra were very similar to those of kerogen and amorphous carbon

spectra obtained from ca. 1.8 Ga microfossils from the Gunflint Formation that are widely held to be biogenic although the authors could not rule out an abiogenic origin for Warrawoona organic matter particularly since they noted similarities in EELS and XANES spectra with Fischer Tropsch-synthesized carbons.

Westall and Rouzaud (2004) analyzed carbonaceous microfossils in 3.3–3.5 Ga cherts from Pilbara Craton and Barberton Greenstone Belts using TEM and Raman spectroscopy. The Raman spectrum was similar to that typically produced by disordered (but not amorphous) mature kerogen. HRTEM analysis revealed an atomic structure of the organic matter consisting of stacks of a few, short, nanometric, wrinkled sheets with relatively wide interspacing, indicating a moderate stage of thermal maturity (apparently consistent with prehnite/pumpellyite grade). Another HRTEM investigation by Rouzaud et al. (2005), who analyzed one sample from the Towers Formation of the Apex basalt in the Warrawoona group, showed the presence of bound large polyaromatic structural units with an overall macromolecular carbon structure which had not reached crystalline graphite but which was similar to a typical very mature marine (Type II) Phanerozoic kerogen.

Derenne et al. (2004) and Skrzypczak et al. (2004) reported in abstracts that solid state $^{13}$C NMR spectroscopy of a Warrawoona Group kerogen isolated from a single chert of the Towers Formation in the Apex basalt showed this to be *highly aromatic* in terms of its bulk carbon chemistry (but also contained some aliphatic chains and C–O or C–N functions). However, the solid state $^{13}$C NMR spectrum actually published by Skrzypczak et al. (2005) for this sample (or a similar sample from the Towers Formation, this is not clarified) contradicts this assessment as the spectrum features a *major peak due to aliphatic carbon* and *a surprisingly weak $sp^2$ carbon band* (aromatic or unsaturated carbon). A significant aliphatic carbon content was apparently consistent with other analyses performed in this study using a combination of Electron Paramagnetic Resonance (EPR) spectroscopy, Fourier transform infrared (FTIR) spectroscopy, and pyrolysis gas chromatography mass spectrometry (Py–GC–MS). The published $^{13}$C NMR spectrum showing abundant aliphatic carbon and heteroatom content (C–O or C–N) is surprising giving the typical thermal maturity and age of Warrawoona sediments (metamorphic grade of prehnite-pumpellyite to lower greenschist facies for Apex cherts at North Pole B deposit barite mine).

The contradictory results from these recent studies indicate the need for the development of a reliable characterization of Archaean kerogens by the combination of complementary bulk structural (elemental analysis and spectroscopic methods) and molecular approaches (following extraction of sediments and fragmentation of kerogen). Obtaining information about the chemical and physical macromolecular structure of insoluble carbonaceous materials is best accomplished with a combination of catalytic hydropyrolysis and solid-state spectroscopic techniques such as Nuclear Magnetic Resonance (NMR) spectroscopy, Fourier transform infrared (FTIR) spectroscopy, and Raman spectroscopy.

FTIR and $^{13}$C NMR spectroscopy are more sensitive in elucidating functional groups of mixtures of aliphatic and aromatic materials, while Raman spectroscopy is more sensitive to elucidating the 2-D and 3-D organization of the carbon network (biperiodic and triperiodic structure) of hydrogen lean kerogens.

Catalytic hydropyrolysis is used instead of standard pyrolysis due to the higher yields of products routinely obtained when using an effective hydrogen donor (Love et al., 1995), which is particularly appropriate for hydrogen-lean carbonaceous materials such as Archaean kerogens. A continuous flow of high-pressure hydrogen ensures that product rearrangements are minimal, thereby suppressing the recombination of pyrolysis products into a solvent-insoluble char and minimizing alteration to organic structures and stereochemistries (Love et al., 1995).

With respect to Archaean sedimentary organic matter, standard pyrolysis procedures do not always discriminate between absorbed and covalently bound organic species. Hydropyrolysis is a temperature-programmed method which facilitates the use of an initial low temperature treatment to drive off residual volatiles (Love et al., 1997; Brocks et al., 2003) which have escaped multi-step solvent extraction. Equally important, as demonstrated already for the highly aromatic and insoluble macromolecular organic matter found in carbonaceous chondrite meteorites (e.g., HyPy studies of Sephton et al., 2004, 2005, in comparison with the Py–GC–MS results of Komiya and Shimoyama, 1996; Remusat et al., 2005, and with the closed-sytem hydrous pyrolysis results of Sephton et al., 1999), HyPy routinely generates higher conversions of kerogen into GC-analyzable products compared with conventional pyrolytic approaches and extends the analytical window to include the larger ring PAH (5–7 ring PAH) products with significantly higher amounts of 3–7 ring PAH compounds detected in general, which are usually discriminated against with standard pyrolysis technique.

This paper extends our preliminary work (Marshall et al., 2004a,b) of Raman spectroscopy and solid state $^{13}$C

NMR spectroscopy of carbonaceous materials isolated from the Strelley Pool Chert.

## 2. Geological setting

The Archaean Pilbara Craton, Western Australia, consists of three granite-greenstone terrains separated by late-tectonic clastic basins. The East Pilbara Granite-Greenstone Terrain represents the ancient nucleus of theraton. It consists of the 3.51–3.0 Ga Pilbara Supergroup of volcanic and sedimentary rocks that has been intruded by a variety of granitic rocks dated between 3.49 and 2.83 Ga (Figs. 1 and 2, Van Kranendonk et al., 2002, 2005). The Pilbara Supergroup consists of four autochthonous groups. The oldest (3.51–3.42 Ga) Warrawoona Group consists of dominantly volcanic and minor sedimentary rocks (Fig. 2). Important sedimentary units in this group include: the ca. 3.49 Ga hydrothermal

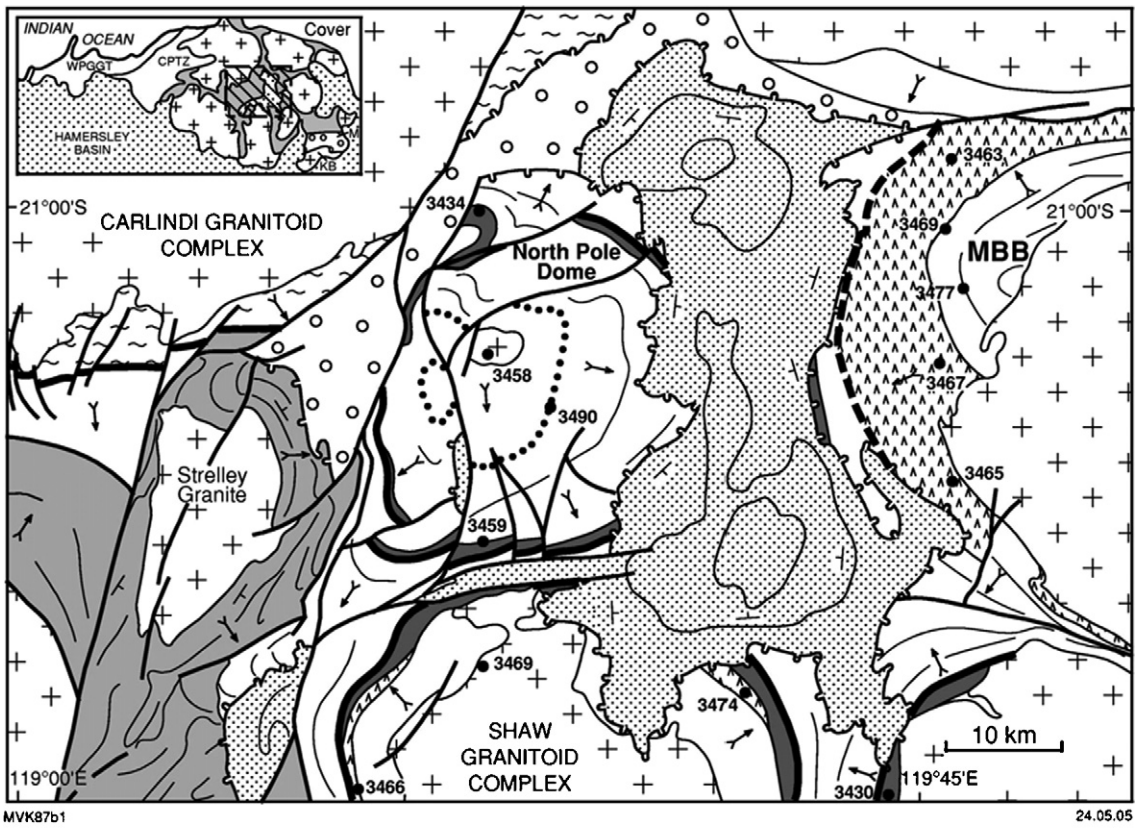


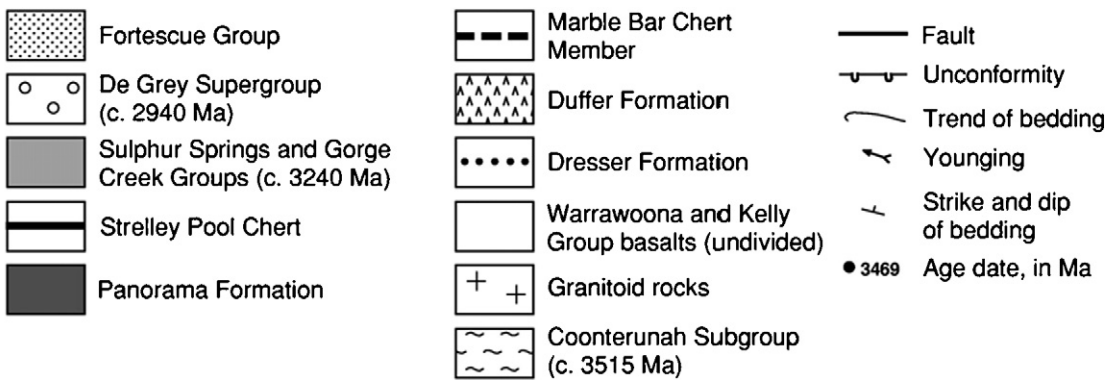


Fig. 1. Geological map of the East Pilbara Granite-Greenstone Terrain, showing important chert horizons. Modified from Van Kranendonk and Pirajno (2004).

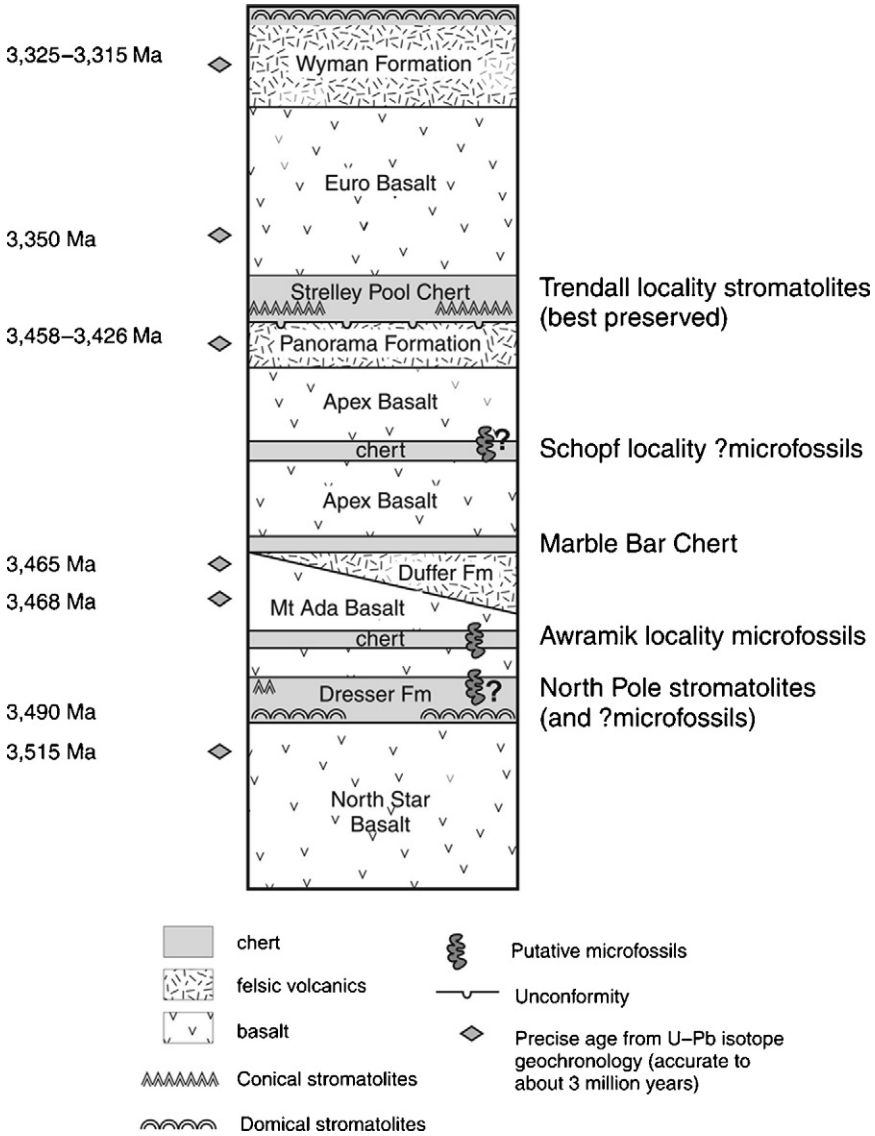


Fig. 2. Simplified stratigraphic column of the Warrawoona and Kelly Groups of the Pilbara Supergroup, showing the stratigraphic position of putative fossiliferous horizons, including the Strelley Pool Chert. See text for further description.

chert-barite units of the Dresser Formation that contain putative stromatolites and microfossils (Walter et al., 1980; Ueno et al., 2004); the Apex Basalt, which contains a chert unit that contains the controversial microfossils described by Schopf (1993) and Schopf et al. (2002), that have been contested by Brasier et al. (2002, 2005) and Garcia Ruiz et al. (2003) and putative microfossils in a thin chert unit in the Mount Ada Basalt (Awramik et al., 1983). These rocks were weakly deformed under low-grade metamorphic conditions and unconformably overlain by the ca. 3.43–3.32 Ga Kelly Group (Van Kranendonk et al., 2005), which consists of a basal chert-carbonate unit known as the Strelley Pool Chert, and the conformably overlying Euro Basalt and Wyman Formation and Charteris Basalt. The Strelley Pool Chert, denoted as SPC, contains putative stromatolites deposited in a shallow marine environment (Lowe, 1980, 1983; Hofmann et al., 1999; Van Kranendonk et al., 2003; Allwood et al., 2004, 2005, 2006a).

Recent mapping has found that the ca. 3.43 Ga SPC is distributed across the 180 km diameter of the East Pilbara Granite-Greenstone Terrain (Van Kranendonk et al., 2002). The chert and carbonate protoliths were deposited during a 75 million year regional hiatus in volcanism between the end of deposition of the Panorama Formation (3.43 Ga) and onset of volcanism in the Euro

Basalt at 3.35 Ga (Fig. 2). The basal contact of the SPC varies along strike from a paraconformity to a high angle unconformity on the Warrawoona Group and ca. 3.46 Ga granites (Buick et al., 1995; Van Kranendonk, 2000; Van Kranendonk et al., 2002).

Common features of the SPC at most localities include: milky white and grey to black, planar to wavy, siliceous laminates; sets of large, radiating crystal splays; and conical stromatolites. The formation has been extensively silicified, in part due to Cainozoic weathering, but largely due to the introduction of silica in low-temperature hydrothermal veins immediately postdating deposition of the unit (Van Kranendonk and Pirajno, 2004). Local areas of well-preserved, carbonate-rich rocks that have not undergone extensive post-depositional silicification contain sedimentological and trace element evidence for primary carbonate and chert deposition in a range of shallow marine to hydrothermal environments (Allwood et al., 2004, 2005, 2006a). In those areas, the sedimentological and trace element evidence also show that at least some of the chert has a primary origin (Allwood et al., 2006a). Samples used in the present study were selected from those areas where primary cherts occur.

### 2.1. Sample localities

The samples used in the present study were collected from outcrops approximately 500 m north of the 'Trendall Locality' (Hofmann et al., 1999) in the southwestern part of the North Pole Dome. In that area, the SPC consists of a ~30 m thick succession of bedded chemical and clastic sedimentary rocks deposited unconformably over 3.46–3.43 Ga greenschist to amphibolite-facies metavolcanic and sedimentary rocks of the Warrawoona Group (Van Kranendonk et al., 2002, 2003). Four members are recognized from base to top in this locality: (1) a basal coarse clastic unit to 2 m thick (Member 1); (2) overlain by up to 20 m of millimeter-laminated and bedded carbonate and chert (Member 2); (3) up to 2 m of bedded black and white chert (Member 3); (4) an upper unit of clastic sedimentary rocks, to 10 m thick (Member 4) (Fig. 3; Allwood et al., 2006a).

Four of the five samples in the present study are from bedded sedimentary black cherts: Sample 140603-5 is from bedded black and white chert in Member 3; Samples 120803-5, 120803-8 and 10904-16 are from bedded black chert with thin ash layers and intraclast microconglomerates in Member 4. In contrast, sample 1904-11 is from black chert matrix in a highly angular chert breccia at the top of Member 4. The latter is interpreted as a probable phreatomagmatic breccia, implying that the

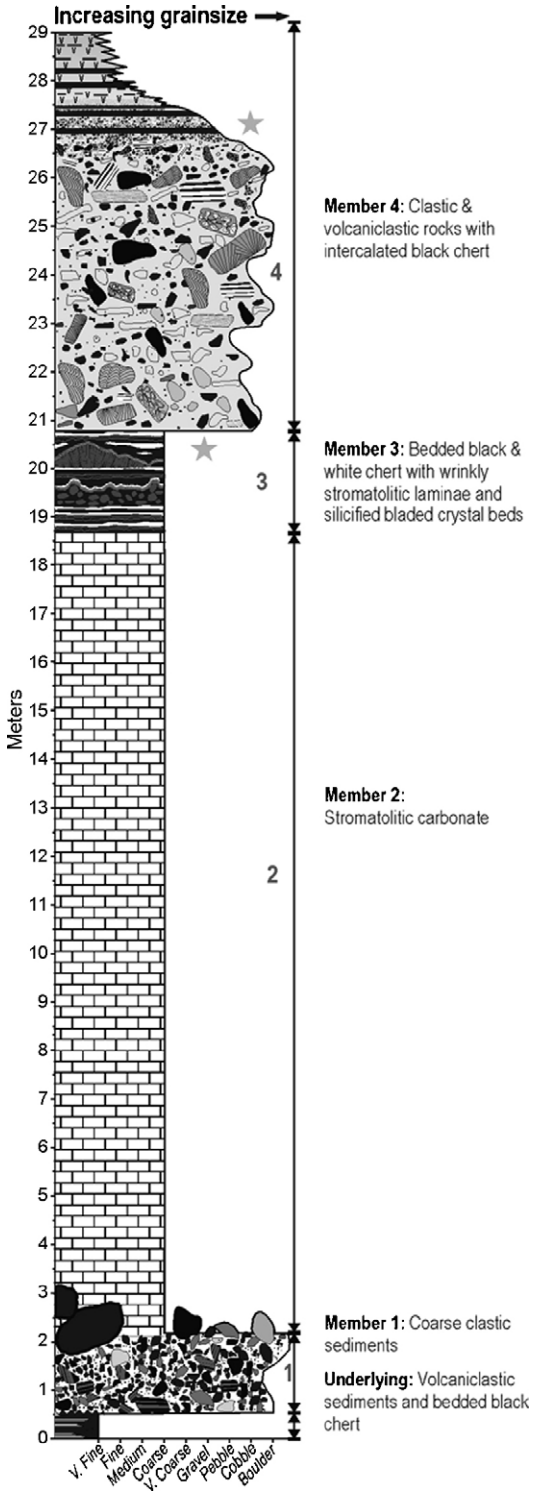


Fig. 3. Generalized stratigraphy of the Strelley Pool Chert in the vicinity of the Trendall Locality. Samples analyzed in the present study were collected from stratigraphic levels marked with a star. Sample 140603-5 is from Member 3. Samples 120803-8, 120803-5, 10904-11 and 10904-16 are from Member 4.

black chert was emplaced after deposition of the original sediment.

## 3. Experimental

### 3.1. Isolation of kerogen

The weathering surfaces (rinds) of the rock samples were removed by rock saw and the internal surfaces of the rock samples were cleaned with dichloromethane to remove possible contamination during sample collecting and sawing. Rock samples were ground to <200 mesh grain size and extracted using soxhlet apparatus in ultra-high purity dichloromethane for 72 h. The isolation of kerogen was conducted by the standard hydrofluoric acid/hydrochloric acid (HF/HCl) extraction procedure (Durand, 1980). Further treatment of the isolated kerogens involved ultrasonic extraction with dichloromethane (×3), then with *n*-hexane (×3). To remove any residual trapped bitumen, the carbonaceous material was swelled twice by ultrasonication in pyridine at 80 °C for 2 h. The pyridine was removed by centrifugation and the kerogen concentrate was further extracted with methanol and then finally with dichloromethane (×3).

The solvent extracted and pyridine swelled kerogens were used for elemental analysis, $\delta^{13}C$ measurements, FTIR spectroscopy, solid state $^{13}C$ NMR spectroscopy, Raman spectroscopy, and HyPy–GC–MS.

### 3.2. TOC and elemental analysis

Total organic carbon (TOC) and Rock-Eval pyrolysis parameters were determined on a Vinci Rock-Eval 6 instrument according to established procedures (Espitalie et al., 1977). Carbon, hydrogen, and nitrogen elemental compositions were determined on a Carlo Erba 1106 instrument.

### 3.3. Bulk carbon isotope ($\delta^{13}C$) measurements

Carbon isotope ratios of ∼1 mg of kerogen in each sample were analyzed by Elemental Analyzer—isotope ratio mass spectrometry (EA-IRMS) using a Europa Roboprep CN elemental analyzer attached to a Finnigan MAT Conflo III and Finnigan MAT 252 mass spectrometer. Stable isotope ratios are expressed using $\delta$ notation, which indicate the difference, in per mil (‰), between the isotope ratio in the sample and an internal reference: $\delta^{13}C$ (‰) = $[(^{13}C/^{12}C_{sample} - {}^{13}C/^{12}C_{standard})/{}^{13}C/^{12}C_{standard}] \times 1000$. The internal reference ($CO_2$) is calibrated against NBS 19, hence the isotope ratios are reported on the VPDB scale (Stalker et al., 2005) with a precision of ±0.2‰.

### 3.4. Fourier transform infrared/attenuated total reflection (FTIR/ATR) spectroscopy

FTIR/ATR spectra were collected using a Bruker IFS66V FTIR spectrometer (Bruker, Karlsruhe, Germany) equipped with a KBr beamsplitter and DLTGS detector. The ATR accessory used was a MIRacle single reflection horizontal ATR (Pike Technologies, Madison, WI) equipped with a composite diamond internal reflection element (IRE) with a 2 mm sampling surface and a ZnSe focusing element. Single-beam spectra of all the samples were obtained and ratioed against a single-beam background spectrum of air to produce a spectrum in absorbance units. The ATR accessory was purged with nitrogen prior to and during acquisition of spectra. Spectra were collected over the region of 4000–600 $cm^{-1}$ with the co-addition of 128 scans at a resolution of 4 $cm^{-1}$.

### 3.5. Solid state $^{13}C$ nuclear magnetic resonance (NMR) spectroscopy

Solid state $^{13}C$ NMR spectra were obtained on a Bruker DRX 200-MHz instrument using cross-polarization (CP) and magic angle spinning (MAS) of 54.7° to the applied field. The kerogens were packed into 4 mm zirconia rotors with Kel-F caps and spun at a speed of 10 kHz. The CP experiments required up to 150,000 transients with a contact time of 1.5 ms and recycle delay of 2 s. Spectra were collected as 1k of data points, zero filled to 4k and then Fourier transformed using a line broadening factor of 50 Hz to obtain the frequency domain spectra. The low field peak of adamantane was employed as a secondary reference (38.3 ppm). Blanks were run on empty rotors to ensure no artifacts were contributed to the spectra. The $f_a$ value is measured directly from the spectra by integrating the signals from 0 to 100 ppm (aliphatic) and 100 to 170 ppm (aromatic) and is defined as: $f_a = C_{Ar}/(C_{Ar} + C_{Ali})$, where $f_a$ is the aromaticity, $C_{Ar}$ is the integrated aromatic signal band between 100 and 170 ppm, $C_{Ali}$ is the integrated aliphatic signal band between 0 and 100 ppm.

### 3.6. Raman spectroscopy

Raman spectra were collected on the extracted isolated kerogen. Since spectral features used to infer the degree of crystallinity of disordered $sp^2$ carbons vary depending on the orientation of the crystallites to the

exciting laser beam, spectra were recorded from 2 to 10 different points in each sample to check the representative nature of the spectra. The Raman spectra were acquired on a Renishaw Raman Microprobe Laser Raman Spectrometer using a charge coupled detector. The collection optics are based on a Leica DMLM microscope. A refractive glass 50× objective lens was used to focus the laser onto a 2 μm spot to collect the backscattered radiation. The 514.5 nm line of a 5 W $Ar^+$ laser (Spectra-Physics Stabilite 2017 laser) orientated normal to the sample was used to excite the sample. The instrument was calibrated against the Raman signal of Si at 520 $cm^{-1}$ using a silicon wafer (1 1 1). Surface laser powers of 1.0–1.5 mW were used to minimize laser induced heating of the kerogens. An accumulation time of 30 s and 10 scans were used which gave adequate signal-to-noise ratio of the spectra. The scan ranges were 1000–1800 $cm^{-1}$ in the carbon first-order region. The isolated kerogens were deposited as a dense layer of about 1 mm thickness, which was pressed with a steel spatula onto a clean aluminum microscope slide and irradiated with the laser to obtain spectra. For details regarding deconvolution and calculation of band areas refer to Allwood et al. (2006b).

### 3.7. Catalytic hydropyrolysis (HyPy)

The extracted kerogens were impregnated with an aqueous solution of ammonium dioxydithiomolybdate $[(NH_4)_2MoO_2S_2]$ to give a nominal loading of 2 wt.% molybdenum. Ammonium dioxydithiomolybdate reductively decomposes in situ under HyPy conditions above 250 °C to form a catalytically active molybdenum sulfide phase. HyPy runs were performed in an open-system temperature-programmed reactor configuration, which is described in detail previously (Love et al., 1995). In this investigation, the catalyst-loaded kerogens (200–600 mg) were initially heated in a stainless steel (316 grade) reactor tube from ambient temperature to 250 °C using a rapid heating rate of 300 °C $min^{-1}$, then to 520 °C at 8 °C $min^{-1}$, using a hydrogen gas pressure of 15 MPa. A constant hydrogen gas flow of 6 $dm^3$ $min^{-1}$, measured at ambient temperature and pressure, through the reactor bed ensured that the residence times of volatiles generated from pyrolysis were of the order of a few seconds. The HyPy products were collected in a silica gel trap cooled with dry ice. For comparison, a middle oil-window-mature Mesoproteozoic rock containing biogenic kerogen (core sediment from Urapunga4 well, 135.0–135.2 m depth, from ca. 1.45 Ga Velkerri Fm, Roper Group, McArthur Basin, Northern Territory, Australia, with Hydrogen Index = 390 mg g $TOC^{-1}$ from Rock Eval pyrolysis and $TOC_{sediment}$ = 7.5 wt.%) was exhaustively pre-extracted with dichloromethane/methanol (93:7, v/v) in a soxhlet apparatus and the extracted residue was subjected to the same catalytic hydropyrolysis treatment.

For two SPC kerogen samples (1904-11 and 1904-16), a sequential dual temperature HyPy approach was performed to discriminate between residual bitumen (released at low temperature) and molecules covalently bound within kerogen (released at high temperature), similar to that used previously (Brocks et al., 2003). In the initial step, catalyst-loaded samples were heated from ambient temperature to 250 °C at 300 °C $min^{-1}$ and then to 330 °C and held there for 10 min using the same hydrogen gas pressures and flow-rates described above to thermovaporize residual volatile components from the sample. The silica gel in the product trap containing the low temperature HyPy products (330 °C) was recovered and the trap was refilled with clean silica gel for the sequential high temperature stage. The residue from this run was then heated up to 520 °C under typical HyPy conditions to cleave covalent bonds in the kerogen to release bound PAH and traces of alkanes trapped in the microporous kerogen matrix. Products from 330 and 520 °C temperature runs were collected and fractionated separately.

Whole hydropyrolysates were recovered from silica gel by elution with dichloromethane–methanol (3:1, v/v) in short glass Pasteur pipette columns and concentrated to smaller volumes under a stream of nitrogen gas. Pre-extracted and activated copper turnings were added to the concentrated solution to remove all traces of elemental sulfur, which is formed from disproportionation of the catalyst during HyPy. Aliquots of whole hydropyrolysates (treated with Cu) were separated by silica gel adsorption chromatography in short glass Pasteur pipette columns into aliphatics (alkanes plus alkenes), aromatics and polars (or N, S, O compounds) by sequential elution with *n*-hexane, *n*-hexane–dichloromethane (3:1, v/v) and dichloromethane–methanol (3:1, v/v), respectively. Whole hydropyrolysates as well as aliphatic and aromatic hydrocarbon fractions were analyzed in detail by gas chromatographic techniques (see Sections 3.8 and 3.9).

To reduce the levels of background contamination in HyPy, a cleaning run was performed before each sample run whereby the apparatus was heated to 520 °C using a rapid heating rate (300 °C $min^{-1}$) under high hydrogen pressure conditions. Experimental blanks, using clean silica gel in the reactor tube instead of a kerogen sample, were regularly performed and the products monitored

and quantified to ensure that trace organic contamination levels were acceptably low.

### 3.8. Gas chromatography (GC) and gas chromatography–mass spectrometry (GC–MS)

Gas chromatography (GC) was performed with a Hewlett-Packard HP6890 gas chromatograph fitted with a flame ionization detector (FID) and a Chrompak CP Sil 5CB capillary column (60 m × 0.32 mm i.d., 0.25 μm film thickness) using He as a carrier gas. The GC oven was programmed at 60 °C (2 min), heated to 315 °C at 4 °C min$^{-1}$, with a final hold time of 25 min. Selected hydrocarbon products in total hydropyrolysates were quantified relative to the $C_{22}$ branched alkane standard, 3-methylhenicosane, from relative peak areas.

Compound detection and identification was performed by GC–MS in full-scan mode on a Hewlett Packard HP6890 gas chromatograph interfaced to a Micromass AutoSpec Ultima magnetic sector mass spectrometer. GC separation was performed on a J&W Scientific DB-1MS capillary column (60 m × 0.25 mm i.d., 0.25 μm film thickness) using He as carrier gas. Samples were injected in splitless mode at 300 °C. The oven was programmed from 60 °C (held for 2 min) to 150 °C at 10 °C min$^{-1}$, then at 3 °C min$^{-1}$ to 315 °C and held isothermal for 24 min. The source was operated in electron ionization (EI) mode at 70 eV ionization energy at 250 °C. The AutoSpec full-scan rate was 0.80 s/decade over a mass range of 50–600 Da and a delay of 0.20 s/decade. Peak identification was based on retention times and mass spectral comparisons with authenticated standards and well-characterized aromatic fractions of coal tar and crude oil (e.g., Kruge, 2000, and references therein).

### 3.9. Gas chromatography–isotope ratio mass spectrometry (GC–IRMS)

Compound-specific stable carbon isotopic compositions were measured on a Finnigan Delta + XL isotope-ratio-mass spectrometer coupled to an Agilent 6890 GC via the Finnigan combustion interface held at 850 °C with a constant oxygen trickle. Extracts were separated using a J&W DB-5 MS 30 m capillary column with 250 μm diameter and 0.25 μm film thickness. The oven temperature program for aromatic fractions was as follows: 40 °C (0.5 min) ramp to 90 °C at 20 °C min$^{-1}$ (2 min hold) ramp to 290 °C at 3 °C min$^{-1}$ then ramp to 320 °C at 20 °C min$^{-1}$ (10 min hold). Samples were evaluated using injections of square peaks of $CO_2$ of known isotopic composition. Due to the complexity of the chromatograms external standards of known isotopic composition were used to estimate error. Error, reported as the root-mean-square error, for 16 individual *n*-alkanes was 0.23‰ for theses analysis. The pooled standard deviation for aromatic fractions was 0.75‰.

## 4. Results and discussion

### 4.1. Petrography

All samples except 1904-11 have a laminated fabric (Fig. 4A), which arises from the preferential alignment of sub-millimetre-sized carbonaceous clots and clasts in a matrix of polygonal microcrystalline quartz (Fig. 4B). The four laminated rock samples come from sedimentary beds and not from cross cutting (post-depositional) veins. The carbonaceous clots and clasts are part of the inherent rock fabric with clasts of silicified rocks or minerals, and the lamination defined

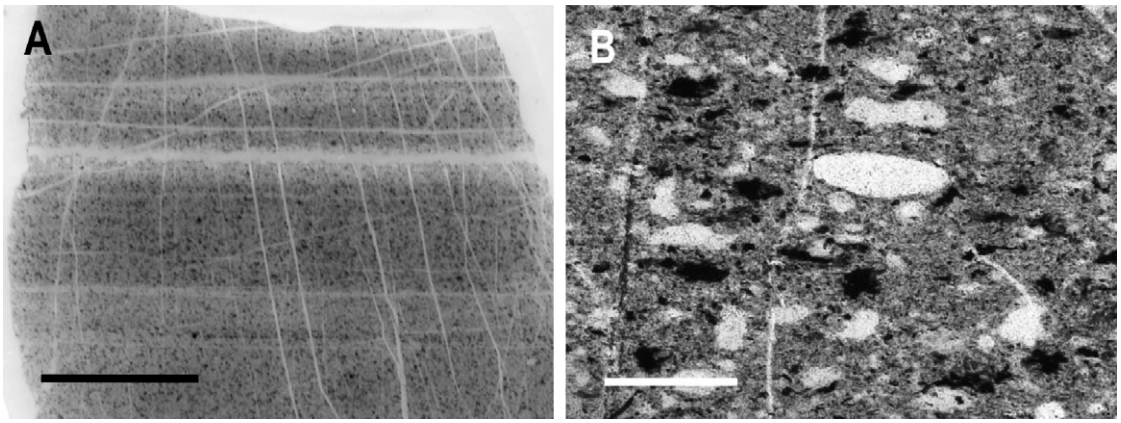


Fig. 4. Sedimentary fabric of representative sample thin sections. (A) Sample 120803-8: laminated fabric defined by the density and alignment of carbonaceous grains and particles in the chert matrix. Scale = 0.5 cm. (B) Sample 140803-2: carbonaceous material (black) occurring as clasts and clots distributed among rounded silicified grains, such as the large pale grain above centre.

by the carbonaceous clasts is continuous to the edges of the sample and is conformable with the larger sedimentary bedding. This attests to the syndepositional origin of the carbonaceous material. In contrast, sample 1904-11 comes from cross-cutting, post-depositional phreatomagmatic breccia matrix and displays no depositional layering. The carbonaceous material in 1904-11 occurs as evenly distributed clots and clasts in a chert matrix. The carbonaceous material in 1904-11 is therefore of post-depositional origin. No microfossils, like those described by Schopf (1993), were observed in our samples.

The kerogen isolated from all the chert samples is black, consistent with the samples having been subjected to a thermal history exceeding 250 °C (Hunt, 1996). This is in agreement with the thermal parameters derived in this study and from previous studies that show the SPC has been affected by post-depositional hydrothermal activity (Van Kranendonk and Pirajno, 2004).

### 4.2. TOC and elemental analysis

The total organic carbon (TOC) contents of the chert samples are low and vary from 0.08 to 0.22 wt.% (Table 1). Bulk atomic H/C ratios for isolated kerogens vary from 0.02 to 0.46 (Table 1). For comparative purposes, terrestrial semianthracite coals have H/C ratios of ∼0.5 and cores of five or six aromatic rings, while anthracites have H/C ratios of ∼0.3 and comprise clusters of greater than 15 aromatic rings. The range in bulk atomic H/C ratios suggests a thermal history variation between the samples with the lower H/C ratios signifying that these have been more thermally altered. Not surprisingly, the most thermally altered sample (1904-11) is the one sample in which the organic matter is not syndepositional but is associated with a cross-cutting breccia matrix.

### 4.3. Bulk kerogen $\delta^{13}C$ measurements

The bulk isotopic $\delta^{13}C$ compositions of kerogens are summarized in Table 1. The bulk $\delta^{13}C$ values vary from −28.3 to −35.8‰. The kerogens from the SPC are depleted in $^{13}C$ to a degree typically ascribed to biological processes. Recently, however (Brasier et al., 2002, 2005; Lindsay et al., 2005; McCollom and Seewald, 2006), the use of bulk carbon isotope compositions for unambiguously assessing biological contributions to carbonaceous material preserved in Archaean rocks have come under intense scrutiny. McCollom and Seewald (2006) have recently shown that the abiotic synthesis of organic compounds ($C_2$–$C_{28}$ *n*-alkanes) under laboratory-simulated hydrothermal conditions can yield organic products depleted in $^{13}C$ to such a degree usually diagnostic of biological isotopic fractionation (−36‰ depletion in organic carbon, in the form of isotopically uniform *n*-alkanes, estimated relative to source carbon dioxide was observed), at least when overall $CO_2$/CO reductive conversions are low. So, additional key evidence from molecular and compound-specific isotopic patterns, as well as spectroscopic characterization, is necessary to differentiate biotic from abiotic carbonaceous inputs to Earth's oldest preserved sediments.

Table 1
The total organic carbon (TOC) contents of Strelley Pool Cherts together with atomic H/C, N/C ratios, and $\delta^{13}C$ measurements for the indigenous organic matter in the samples investigated in this study

| Samples | TOC (wt%) | H/C | N/C | $\delta^{13}C$ (‰) |
|---|---|---|---|---|
| 1904-11 | 0.22 | 0.02 | – | −34.0 |
| 1904-16 | 0.17 | 0.14 | 0.02 | −35.0 |
| 140603-5 | 0.13 | 0.33 | – | −35.2 |
| 120803-5 | 0.08 | 0.46 | – | −28.3 |
| 120803-8 | 0.21 | 0.08 | – | −35.8 |

### 4.4. Fourier transform infrared/attenuated total reflection (FTIR/ATR) spectroscopy

For brevity, since the spectra are essentially featureless they are not displayed here. For all samples (Table 1), a low H/C atomic ratio can be observed, indicating a highly aromatic character. All spectra display a lack of aliphatic C–H stretching modes in the 3000–2700 $cm^{-1}$ region and the lack of an absorption at 720 $cm^{-1}$ corresponding to skeletal vibrations in long polymethylenic chains, which is consistent with the low H/C atomic ratios. There is also, a lack of any absorptions arising from carbon–nitrogen and carbon–oxygen functionalities. The only absorptions in the spectra are weak Si–O vibrational modes at ∼1000 $cm^{-1}$, due to residual silica in the kerogen isolate. Furthermore, it is noteworthy that the spectra of these carbonaceous materials show a moderately flat baseline with no absorptions from 4000 to 750 $cm^{-1}$, and a rapid rise in absorbance from 750 to 500 $cm^{-1}$, which is typically produced by strong electronic absorption that arises from condensed polyaromatic networks similar to large polycyclic aromatic hydrocarbon (PAH) structures such as disordered $sp^2$ carbons (Painter et al., 1985). This is in disagreement with the FTIR spectroscopy results obtained by Derenne et al. (2004) and Skrzypczak et al. (2004, 2005) in which they reported significant aliphatic absorptions, C–O, or C–N bonding, and which is surprising given that their sample has undergone prehnite-pumpellyite to

lower greenschist facies metamorphism and given that the samples have been buried for 3.4 Ga.

### 4.5. $^{13}C$ Nuclear magnetic resonance (NMR) spectroscopy

A representative solid state $^{13}C$ NMR spectrum acquired from the isolated kerogen is shown in Fig. 5.

This is a typical CP MAS $^{13}C$ solid state NMR spectrum acquired from thermally overmature kerogens, in which the spectra have been collected under long accumulation times, but still show poor signal to noise (S/N). The spectrum shows a resonance band from 100–150 ppm, centered at approximately 125 ppm that corresponds to the presence of aromatic carbons which may be protonated (linked to a hydrogen atom) or non-protonated (most probably carbon substituted), and which we will refer to in total as aromatic carbon. In addition to the main aromatic carbon resonance, a slight shoulder can be observed at approximately 150 ppm. This is attributed to oxygen substituted aromatic carbons such as phenols and phenyl ethers. At the lower frequencies between 0 and 90 ppm, there is one small resonance centered at approximately 65 ppm which could be one of two possibilities: the resonance is an artifact or the resonance could be assigned to the presence of methoxy (O–$CH_3$) $sp^3$ bonded carbon functional group. It is more likely that this resonance at 65 ppm is an artifact of spectral acquisition.

It is clear that, qualitatively, aromatic carbon is the greatest constituent in the macromolecular network of these kerogens. The fraction of aromatic carbon ($f_a$), measured in this investigation for our samples varies from 0.90 to 0.92 (i.e., 90–92% of total carbon is aromatic). These $f_a$ values derived from the solid-state $^{13}C$ NMR (CP MAS) spectra are what would be expected given the H/C ratios obtained (0.02–0.46) from these samples. The H/C ratio's <0.5 suggest that the macromolecular network consists of very large PAH clusters on average (>15 aromatic rings), which is in agreement with the $f_a$ values. Furthermore, these $f_a$ values are indicative of kerogen that has undergone significant metamorphism or hydrothermal alteration, which is in agreement with the post-depositional hydrothermal activity of the SPC. However, it is worth noting that CP MAS solid-state $^{13}C$ NMR spectroscopy, which utilizes transfer of magnetization from abundant $^{1}H$ to dilute $^{13}C$ spins to increase signal/noise in $^{13}C$ spectra, can generally discriminate against carbons distant from protons. Non-protonated carbons in the core of the large ring clusters are, therefore, likely to be underestimated to some degree, especially when contact times of 1 ms or less are used in cross polarization pulse sequences (e.g., as noted by Franz et al., 1992).

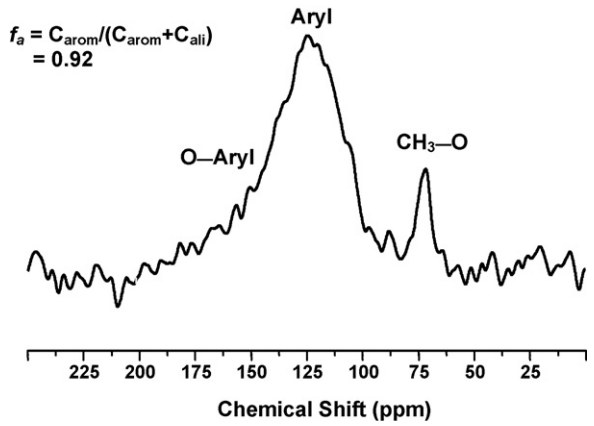


Fig. 5. A representative solid state $^{13}C$ NMR spectrum acquired from the isolated insoluble carbonaceous material (sample 120803-8).

Solid state $^{13}C$ NMR spectroscopy and FTIR spectroscopy shows that the kerogen from the Strelley Pool Chert is highly aromatic and contains little aliphatic C–H, carbon–oxygen C–O, or carbon–nitrogen C–N functionality. This is in stark contrast to the $^{13}C$ NMR spectrum shown for an Apex chert kerogen from Warrawoona Group in Skrzypczak et al. (2005), containing abundant aliphatic carbon despite the high thermal maturity and Archaean age of their sample. Furthermore, it is difficult to invoke a highly aliphatic macromolecular structure (no matter how cross-linked and branched) as being an appropriate model for the kerogen with an atomic H/C ratio of <0.5, given the need for an overall self-consistent H and C balance.

### 4.6. Raman spectroscopy

Raman spectroscopy has been used since the early 1970s for the study of carbonaceous materials. For an extensive review, on Raman spectroscopy of carbonaceous materials refer to Dresselhaus and Dresselhaus (1982 and references therein). For an extensive discussion highlighting salient features in understanding band assignments acquired from kerogens, particularly from the SPC, refer to Allwood et al. (2006b). For brevity, the Raman spectra are not shown for all the samples but only for the two samples with the greatest spectral difference. The stacked spectra shown in Fig. 6 show pronounced bands at 1350 (D band) and 1600 $cm^{-1}$ (G band, which is a combination of the G and D′ bands) in the first-order region, while the second-order region contains a non intense S1 band at 2700 $cm^{-1}$. Little to no 3-D structural ordering is present in these samples,

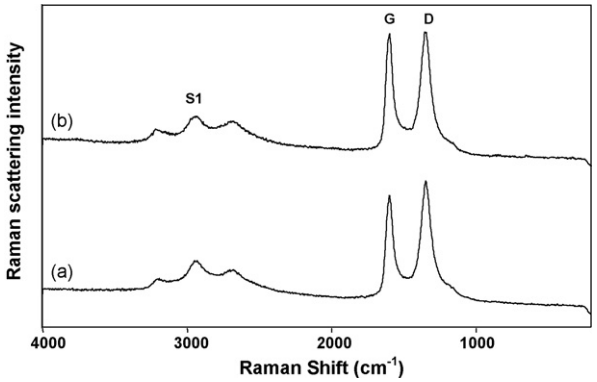


Fig. 6. Stacked Raman spectra are shown for the carbonaceous material isolated from (a) 1904-11 and (b) 120803-8, which shows pronounced absorptions at 1350 (D band) and 1600 $cm^{-1}$ (G band which is a combination of the G and D′ bands) in the first-order region and the second-order region contains a non intense S1 band at 2700 $cm^{-1}$. Note the D band intensity is greater for the spectrum acquired from 1904-11.

which is shown by the low band intensity in the second-order region (Lespade et al., 1982). Therefore, isolated kerogen from the SPC consists of small crystallites with biperoidic structure.

Minor differences in the intensities of the D band with respect to the G band can be observed for the two spectra. The D band intensity increases relative to the G band intensity, and the intensity of the D4 band gradually declines. These changes may reflect the increasing enlargement of polyaromatic structures and accompanying loss of peripheral hydrogen, which occurs during the conversion of polyaromatic structures to graphite (Negri et al., 2002). The width and relative band areas of the G and D lines vary with structural evolution and thus, can be used as an index of metamorphic alteration (e.g., Wopenka and Pasteris, 1993; Jehlicka et al., 2003; Beyssac et al., 2002, 2003; Quirico et al., 2005 and references therein). It can be noted that the spectrum acquired from the isolated kerogen from sample 1904-11 has a greater intensity of the D band, which corresponds to a more severe thermal history. The band becomes progressively narrow and increases in height relative to the G band, where upon increasing thermal maturity the D band decreases again, whereas the S bands increase in intensity representing the graphitization of organic matter. The Raman spectra obtained from these samples reveals that the kerogen has a low degree of 2-D structural organization and can be compared with other spectra of carbonaceous material taken from chlorite up to biotite metamorphic zones (e.g., Wopenka and Pasteris, 1993; Jehlicka et al., 2003 and references therein) representing lower to mid Greenschist facies (Yui et al., 1996), indicating peak temperatures between ~300 and 400 °C through to 400–500 °C (Bucher and Frey, 1994).

The G band full-width at half-maximum (FWHM), $I_{D1}/I_G$ ratio, and $I_{D1}/(I_{D1}+I_G)$ ratio has been shown to correlate with the amount of structural disorder (Beny-Bassez and Rouzaud, 1985; Cuesta et al., 1994 and references therein), therefore these parameters were used to ascertain the degree of structural order between the samples. Carbonaceous solid materials (coals, kerogens, charcoals, cokes, etc.) contain crystalline particles (crystallites) of the order of nanometers in diameter, composed of graphite-like layers/aromatic clusters arranged turbostratically. It is now generally accepted that the relationship between the integrated intensity ratio $I_{D1}/I_G$ and the microcrystalline planar size $L_a$ shows inverse proportional behavior. By calibration against the in-plane crystallite size ($L_a$) measured by X-ray diffraction, it has been shown that the ratio of Raman band intensities, $R = I_{D1}/I_G$, is inversely proportional to the average value of $L_a$ (Tuinstra and Koenig, 1970; Knight and White, 1989). The $L_a$ measurements derived from Raman analyses are calculated using: $L_a = 44[I_{D1}/I_G]^{-1}$ (nm). Where the value of 44 nm is used for an excitation wavelength of 514.5 nm, and $L_a$ is the size of the crystallite. This relationship holds for a wide range of $sp^2$-bonded carbons over the range of $2.5 < L_a < 300$ nm (Ferrari and Robertson, 2002). In addition, it must be noted that also this relationship depends on the nature of the precursor (Beny-Bassez and Rouzaud, 1985). Nonetheless, despite these limitations, it is worth investigating this parameter here.

The degree of structural organization can be further mathematically quantified by using the $I_{D1}/I_G$ and $I_{D1}/(I_{D1}+I_G)$ ratios and further to delineate any minor differences between the samples. The $I_{D1}/I_G$ and $I_{D1}/(I_{D1}+I_G)$ ratios range from 1.07 to 1.37 and 51.8 to 57.8%, respectively (Table 2). The $I_{D1}/(I_{D1}+I_G)$ ratio is known to be a sensitive characterization of disorder in

Table 2
Bulk structural parameters obtained from Raman spectroscopic analysis and molecular parameters derived from HyPy of the kerogens from the Strelley Pool Chert

| Samples | $I_{D1}/I_G$ | $I_{D1}/(I_{D1}+I_G)$ (%) | $L_a$ (nm) | MeP/P |
|---|---|---|---|---|
| 1904-11 | 1.08 | 51.9 | 40.7 | 0.18 |
| 1904-16 | 1.07 | 51.8 | 41.1 | 0.24 |
| 140603-5 | 1.28 | 56.0 | 34.4 | 0.73 |
| 120803-5 | 1.37 | 57.8 | 32.1 | 0.86 |
| 120803-8 | 1.17 | 53.0 | 37.6 | 0.37 |

$I_{D1}/I_G$ = intensity ratio of the D and G bands, $I_{D1}/(I_{D1}+I_G)$ = structural disorder ratio, $L_a$ = crystallite diameter, MeP/P = summed methylphenanthrenes /phenanthrene ratio

carbonaceous materials; the higher the ratio, the greater the degree of structural disorder. $I_{D1}/(I_{D1}+I_G)$ values ranging from 51.8 to 57.8%, as measured in this investigation, indicate structurally disordered carbonaceous material. The dimensions of the graphitic domains or polyaromatic cluster size ($L_a$) range from 32.1 to 41.1 nm (Table 2) which would suggest the graphitic domains in these carbonaceous materials involve approximately 15–25 PNA units.

The ranges between the Raman parameters delineate a thermal trend between the samples. It can be observed from the H/C ratios (Table 1), $I_{D1}/I_G$, $I_{D1}/(I_{D1}+I_G)$, and $L_a$ (Table 2) that a thermal trend can be delineated from most to least altered: 1904-11, 1904-16, 120803-8, 140603-5, and 120803-5. Fig. 7 shows cross-plots of H/C atomic ratios versus $I_{D1}/I_G$, $I_{D1}/(I_{D1}+I_G)$, and $L_a$. These cross-plots illustrate correlations between Raman parameters of measuring structural disorder of the macromolecular network ($I_{D1}/I_G$ and $I_{D1}/(I_{D1}+I_G)$), and diameter of crystallite domains ($L_a$), with H/C atomic ratios.

The carbon first-order spectra for these isolated kerogens are typical spectra obtained from disordered $sp^2$ carbons, and have a similar line-shape to the spectra acquired by Brasier et al. (2002, 2005). The results and subsequent interpretation clearly show that the organic matter in the Warrawoona cherts are not graphitic as previously reported but are formed of nanometric polyaromatic domains. These results are also in agreement with those reported by Rouzaud et al. (2005). Geochemical maturation or metamorphism of almost all naturally occurring organic matter, whether biological or abiological (e.g., alkanes synthesized from FTT processes) in origin, has been proposed to give rise to similar resultant thermally stable products—covalently crosslinked aromatic hydrocarbons and other aromic subunits that that get transformed and condensed through carbonization and graphitization (Lindsay et al., 2005). So, Raman spectroscopy of over-mature carbonaceous material cannot provide definitive evidence of biogenicity by itself (Pasteris and Wopencka, 2003).

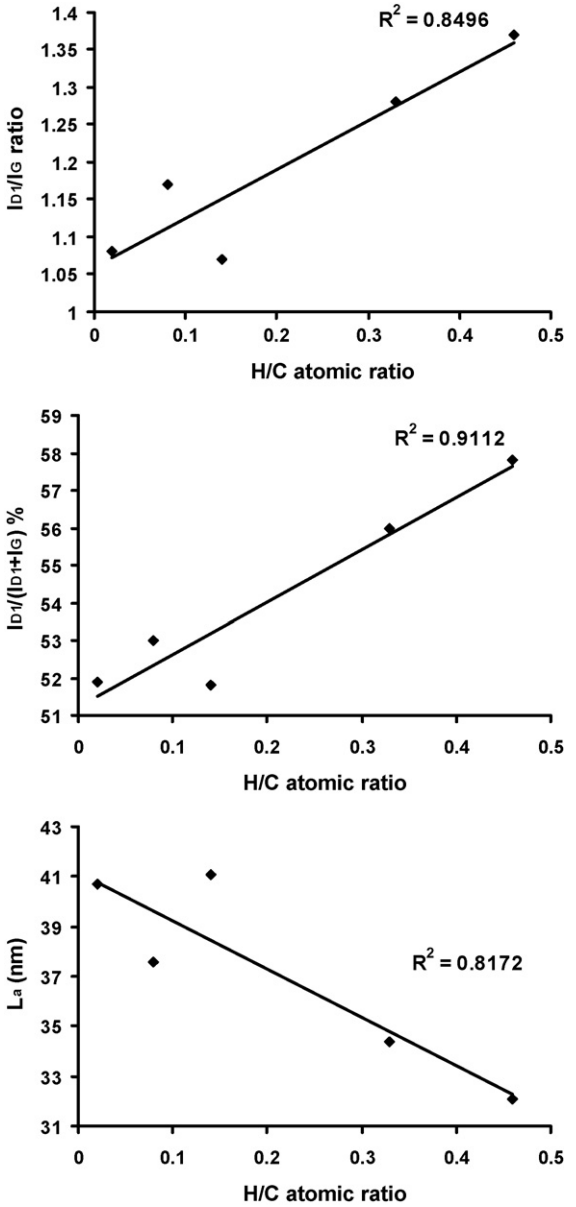


Fig. 7. Cross-plots of atomic H/C ratios produced from elemental analysis vs. $I_{D1}/I_G$, $I_{D1}/(I_{D1}+I_G)$, and $L_a$ parameters obtained from laser Raman specroscopy of Strelley Pool Chert kerogens.

### 4.7. Catalytic hydropyrolysis (HyPy)

Fig. 8 displays representative TICs (Total Ion Chromatograms) of polyaromatic hydrocarbon (PAH) fractions prepared from hydropyrolysates for samples SPC 1904-11 and 1904-16. For these samples, an initial HyPy treatment up to 330 °C was performed to remove any residual bitumen prior to this high temperature run (to 520 °C). Over 99 wt.% of aromatic hydrocarbons were released in the latter high temperature step (Table 3) and so we are confident that, in general, the aromatic compounds reported represent genuine kerogen-bound molecular constituents. The SPC hydropyrolysates contain a diverse range of 1–7-ring PAH compounds, with phenanthrene (3-ring) or pyrene (4-ring) PAH as the major components. Although the chromatograms are complex, the main PAHs do not possesss long and highly branched alkyl side-chains and $C_1$- and $C_2$-substituted PAHs are quantitatively the dominant alkylated forms.

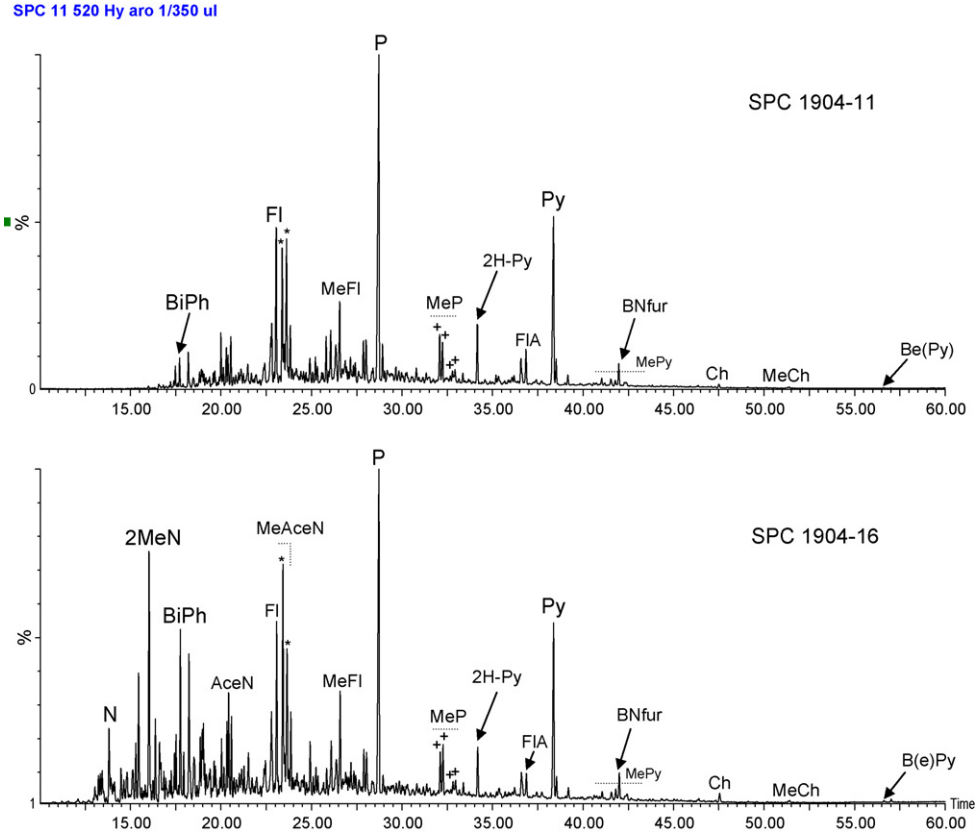


Fig. 8. Total ion chromatogram (TIC) of aromatic hydrocarbons generated from HyPy of 2 SPC kerogen concentrates: (top) SPC 1904-11 (after an intial HyPy pre-treatment to 330 °C to remove residual bitumen), and (bottom) SPC 1904-16 (after an intial HyPy pre-treatment to 330 °C to remove residual bitumen). Preservation of the most volatile aromatics after fractionation of total pyrolysates is best for sample SPC 1904-16. N, naphthalene, 2 MeN, 2-methylnaphthalene, BiPh, 1,1′-biphenyl; AceN, acenaphthene; Fl, fluorine; MeAceN (*), methylacenaphthenes; MeFl, methylfluorenes (+di-/tetra-hydro phenanthrenes + dimethlyacenaphthenes); P, phenanthrene; MeP, methylphenanthrenes; 2H-Py, dihydropyrene; FlA, fluoranthene; Py, pyrene; BNfur, benzonaphthofuran; Ch, chrysene; MeCh, methylchrysene; B(e)Py, benzo(e)pyrene.

The PAH profiles are fairly similar to those observed by Brocks et al. (2003) from HyPy of 2.5 Ga kerogens from Hamersley Group (W. Australia) but the retention of volatile components in this study is superior because of the recent development of a more efficient silica gel product trap (Meredith et al., 2004) rather than a coiled trap containing no adsorbent.

Table 3
Yields of selected saturated and aromatic hydrocarbon products (ppm TOC) generated from sequential dual temperature HyPy of Strelley Pool Chert kerogens 1904-11 and 1904-16

| Sample | Final HyPy $T$ (°C) | $\sum nC_{14} - nC_{20}$ | Phenanthrene | Pyrene |
|---|---|---|---|---|
| 1904-11 | 330 | 102.1 | 0.6 | 0.1 |
| | 520 | 760.1 | 252.1 | 92.4 |
| 1904-16 | 330 | 673.7 | 1.2 | 0.1 |
| | 520 | 1666.1 | 290.9 | 100.0 |

The principal bound PAH released by HyPy have stable carbon isotopic ($\delta^{13}C$) signatures between −29 and −36‰ which when averaged are slightly $^{13}C$-enriched in comparison to the bulk kerogen values (Table 4). This implies that the intractable larger PAH clusters (10–15 ring) comprising the bulk of the kerogen matrix are $^{13}C$-depleted by 0–6‰ in comparison with the quantitatively minor 1–4 ring PAH components and this likely results from preferential incorporation of $^{12}C$ during fusion of aromatic rings into larger structural units during kerogen maturation.

Fig. 9 is a summed ion chromatogram (SIC) of the SPC hydropyrolysate for sample 120803-5 that reveals the dominant parent PAH distribution (non-alkylated) in the aromatic fraction of the hydropyrolysate. The hydropyrolysates shows the presence of naphthalene, phenanthrene, methylphenanthrene, fluoranthene, pyrene, methylpyrene, chrysene, methylchrysene, benzo[ghi]perylene, benzo[e]pyrene, and up to

Table 4
Compound-specific stable carbon ($\delta^{13}C$) isotopic composition (‰ vs. PDB) of selected aromatic compounds released from high temperature HyPy of Strelley Pool kerogens 1904-11 and 1904-16 as determined by GC–IRMS analysis

| Sample | Kerogen | BiPh | MeAceN[a] | P | FlA | Py | BNfur |
|---|---|---|---|---|---|---|---|
| 1904-11 | −34.0 | n.d. | n.d. | −32.9 (0.04) | −31.4 (1.31) | −35.8 (0.12) | n.d. |
| 1904-16 | −35.0 | −29.3 (0.21) | −31.0 (0.47) | −30.5 (0.55) | −29.6 (0.85) | −32.9 (0.16) | −31.1 (0.32) |

BiPh, 1,1′-biphenyl; MeAceN, methyacenaphthenes; P, phenanthrene; FlA, fluoranthene; Py, pyrene; BNfur, benzonaphthofuran. Values in parentheses indicate standard deviation from 2 or more analyses.
[a] Average of two resolvable peaks.

(7-ring PAH) coronene. While aromatic compounds of up to 7-ring PAH could be observed in hydropyrolysate of the 2 samples with highest H/C ratio (120803-5 and 140603-5) only 1–5 ring PAH could be produced for the more recalcitrant kerogens (1904-11, 1904-16 and 120803-8). The total PAH profiles for SPC and Urapunga4 kerogens exhibit the same characteristic features (Fig. 10) and are similar to, allowing for relative thermal maturity differences, the aromatic hydrocarbon distributions reported previously from HyPy of other mature Mesoproterozoic Roper Group kerogens (Brocks et al., 2003) and overmature late Archaean (ca. 2.5–2.7 Ga) marine kerogens from the Hamersley Province, Pilbara Craton (Brocks et al., 2003; Eigenbrode, 2004). The thermally less mature Urapunga4 aromatics, not surprisingly, exhibit a greater degree of alkylation than for SPC kerogens. The aromatic profiles obtained here are fairly distinct from those generated from HyPy treatment of the insoluble carbonaceous material found in Murchison meteorite (Sephton et al., 2004, 2005) and overall HyPy conversions are considerably lower than for Murchison also.

Detailed analyses of aromatic fractions generated for the SPC samples showed that there were distinct differences in molecular profiles, particularly the ratio of alkylated/non-alkylated PAH, which were consistent with the maturity ordering of the kerogens. Fig. 11 displays a combined *m/z* (178 + 192) ion chromatogram showing the distribution and abundance of the methylphenanthrene isomers and phenanthrene for 3 SPC kerogen hydropyrolysates. Fig. 12 shows a cross-plot of total methylphenanthrenes/phenanthrene (MeP/P) ratio for all the SPC kerogens investigated illustrating a range of decreasing MeP/P values which correlates ($r^2 = 0.9190$) well with decreasing atomic H/C ratios. A more severe thermal history results in more thermal cracking and loss of alkyl substituents of PAH constituents and produces a lower abundance of methylphenthrenes relative to parent phenanthrene. The Mesoproterozoic Urapunga4 kerogen, not surprisingly,

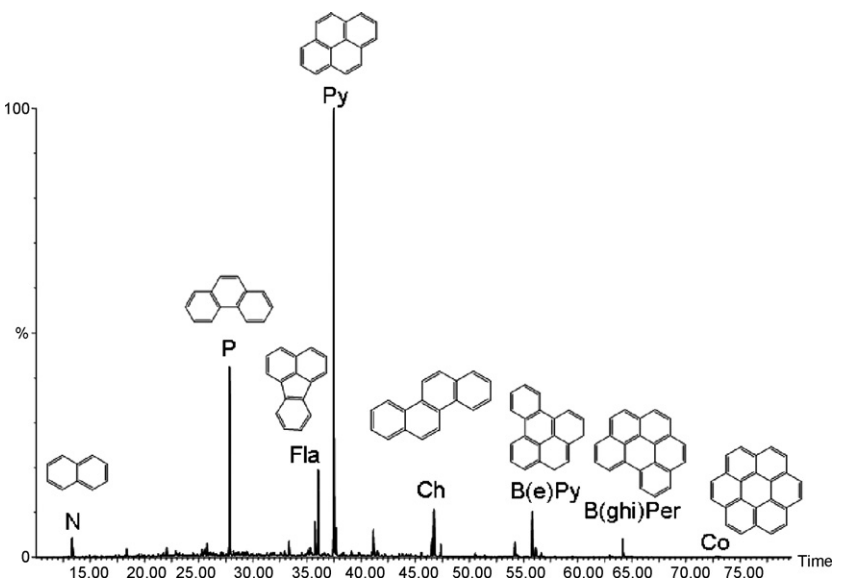


Fig. 9. Summed ion chromatograms (*m/z* 128 + 178 + 202 + 228 + 252 + 276 + 300) showing the main parental PAH present in a SPC hydropyrolysate for sample 120803-5.

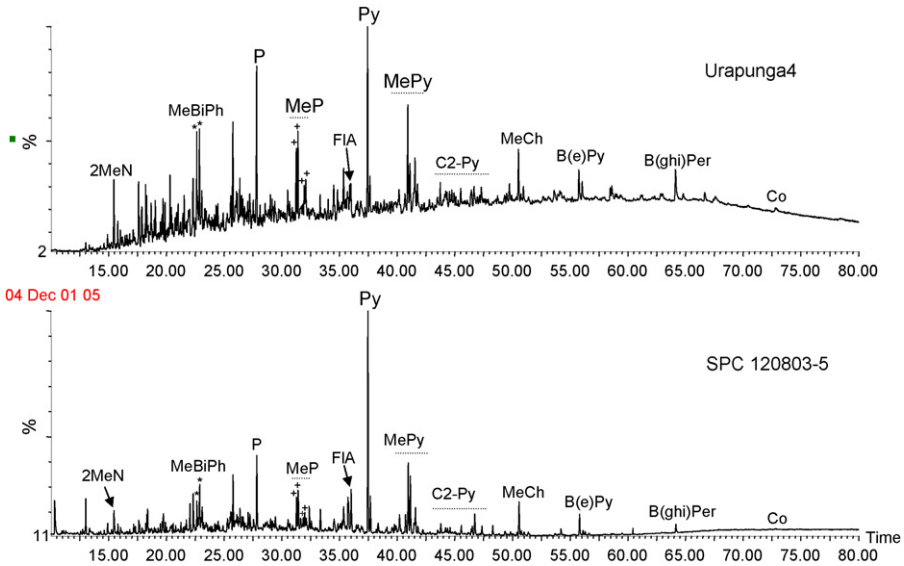


Fig. 10. Total ion chromatogram (TIC) of the total aromatic compounds generated from HyPy of the insoluble organic matter in SPC 120803-5 (the least thermally altered SPC kerogen with the highest atomic H/C) in comparison with those released from the Mesoproterozoic Urapunga4 kerogen. 2 MeN, 2-methylnaphthalene; MeAceN (*), methylacenaphthenes; MeFl, methylfluorenes (+di-/tetra-hydro phenanthrenes + dimethlyacenaphthenes); P, phenanthrene; MeP (+), methylphenanthrenes; FlA, fluoranthene; Py, pyrene; MePy, methylpyrenes; C2-Py, C2-alakylated pyrenes; MeCh, methylchrysene; B(e)Py, benzo(e)pyrene; B(ghi)Per, benzo(ghi)perylene; Co, coronene.

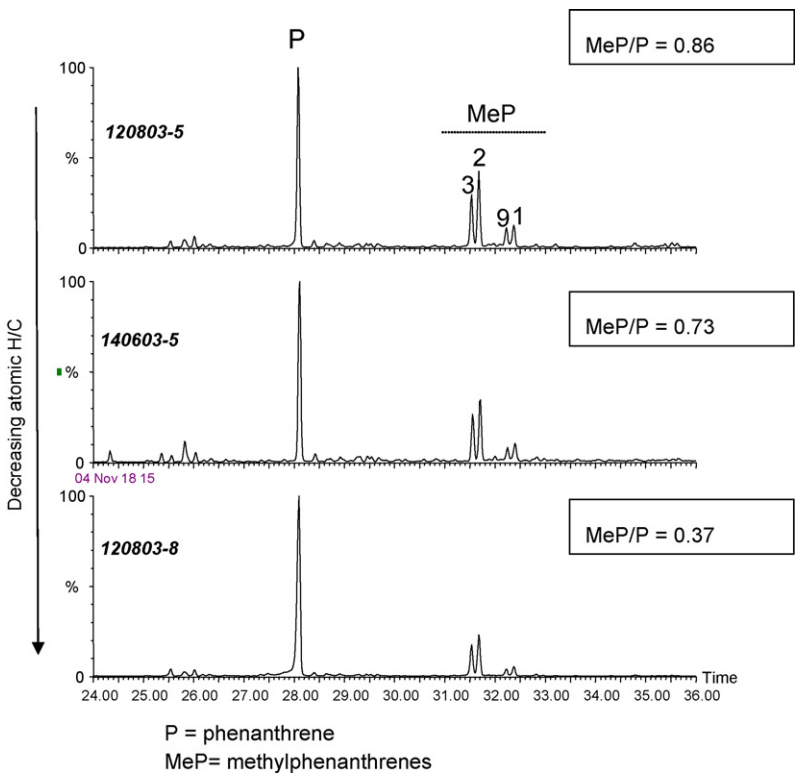


Fig. 11. Summed ion chromatograms (*m*/*z* 178 + 192) showing phenanthrene and methylphenathrenes released from HyPy of 3 SPC kerogens. Numbers (1,2,3,9) refer to the position of the methyl-substituent on phenanthrene.

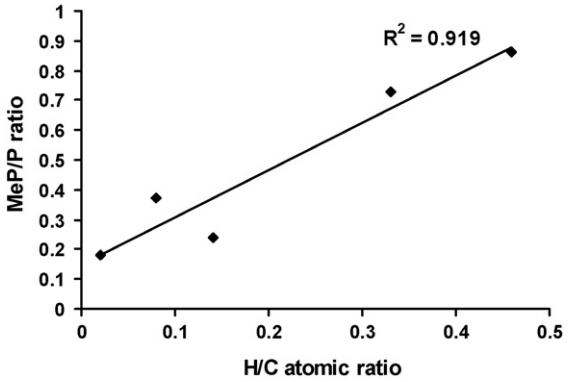


Fig. 12. Cross-plot of atomic H/C atomic ratio vs. the molecular MeP/P (summed methylphenanthrenes/phenanthrene) parameter generated from HyPy treatment of SPC kerogens.

generated a higher value of MeP/P of 1.37 compared with all the SPC kerogens. Significantly, for the first time we have demonstrated a good correlation between bulk structural and molecular parameters for the insoluble carbonaceous material: the bulk structural information being derived from Raman spectroscopy (measurement of structural disorder of macromolecular network and crystallite dimensions) of intact kerogens correlating with the degree of alkylation of aromatic hydrocarbon (e.g., MeP/P) units obtained from HyPy fragmentation of the kerogens (Fig. 13).

Detectable amounts of alkanes, exhibiting a mature distribution (Fig. 14) were observed in all hydropyrolysates and *n*-alkanes up to *n*-$C_{23}$ are evident in TICs. Much higher yields of aliphatic products (alkanes plus alkenes) were released from HyPy treatment of the Mesoproterozoic Urapunga4 kerogen (138 mg g $TOC^{-1}$ of total aliphatics) and in this case this is largely the result of covalent bond cleavage of bound aliphatic components of the kerogen. This is confirmed from the hopane isomer patterns released (*m/z* 191 ion chromatogram) and the detection of a homologous series of *n*-alk-1-enes, whose carbon number distribution, matches that of the corresponding *n*-alkane products (comparing *m/z* 83 and 85 ion chromatograms).

It is significant, however, that the proportions of monomethyl-branched to linear alkanes is similar for both SPC and the Mesoproterozoic kerogen (Fig. 15) and both contain only trace amounts of pristane and phytane. The quantities of *n*-$C_{14}$–*n*-$C_{20}$ alkanes released from sequential dual temperature HyPy treatment of SPC kerogens generally constitute less than 0.3 wt.% of the kerogen matrix (Table 3) and most were released at high temperature following a preliminary low temperature pretreatment (to 330 °C). It was observed that

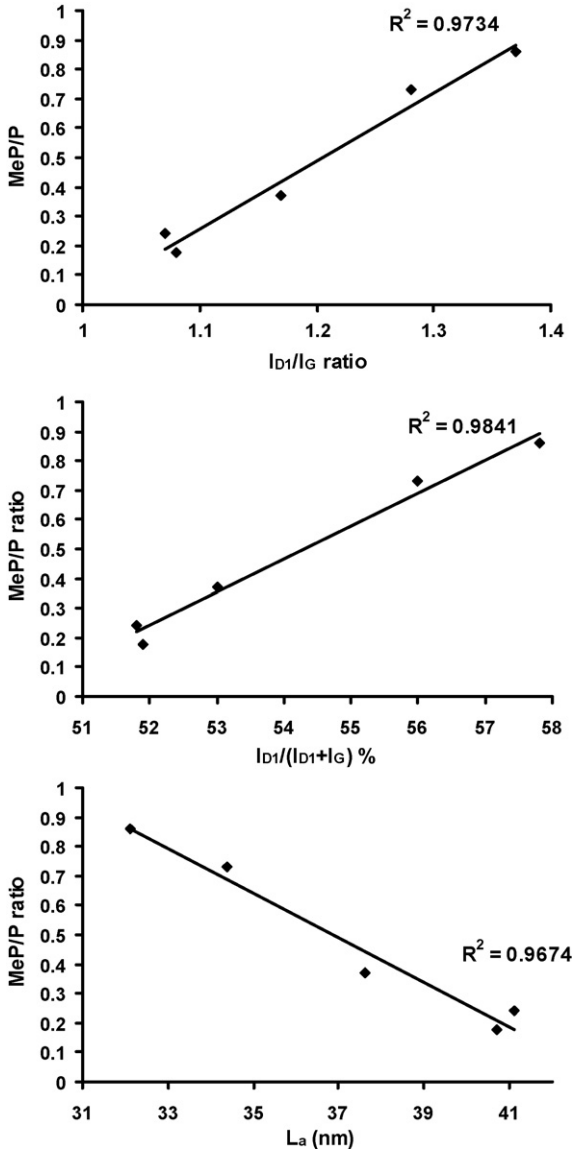


Fig. 13. Cross-plots of MeP/P (summed methylphenanthrenes/phenanthrene) ratio from HyPy vs. $I_{D1}/I_G$, $I_{D1}/(I_{D1}+I_G)$, and $L_a$ structural parameters from Raman spectroscopy.

these alkanes were proportionally more abundant relative to aromatic constituents in chromatograms obtained for the most recalcitrant kerogen samples with the lowest atomic H/C ratios. The alkane products were most likely trapped in closed micropores of the kerogen, so not covalently bound but still not accessible to solvent extraction, and were only released after disruption of the host matrix by cleavage and heating to high temperature during HyPy treatment. The lack of any appreciable alkene content (formed from dehydrogenation reactions that accompany bond cleavage and which can be identi-

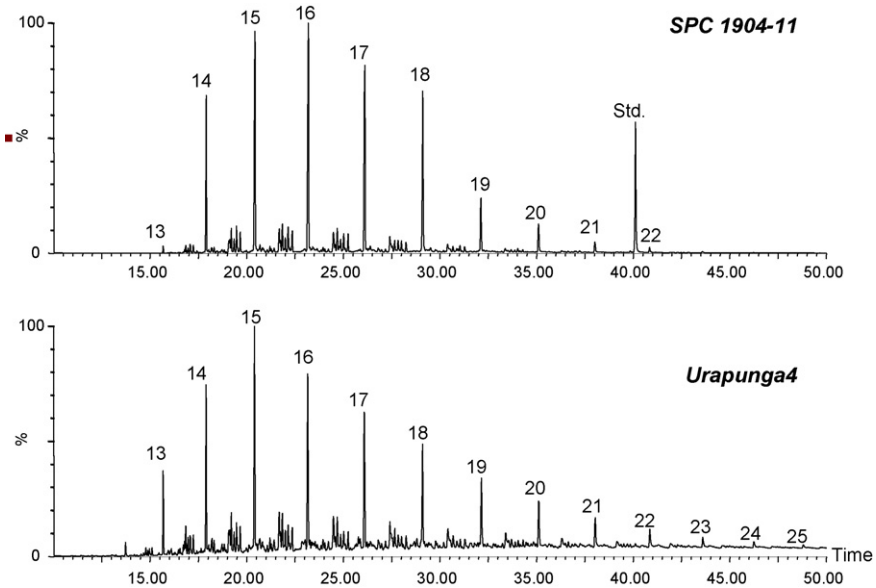


Fig. 14. *m/z* 85 ion chromatograms for SPC 1904-11 and Urapunga4 (Mesoproterozoic) HyPy products, showing similar distributions of *n*-alkanes and methyl-branched alkanes (MMAs). Numbers (13–25) refer to the carbon chain length of *n*-alkanes. Not surprisingly, the *n*-alkane profiles for the less mature Urapunga4 sample extend to higher carbon numbers, although this may be at least partially a source effect.

fied even in very low levels relative to *n*-alkanes by *m/z* 83 or 97 ion chromatograms) for SPC HyPy products supports this interpretation. The alkanes released from SPC kerogens are unlikely to be contaminants because they are largely (>70 wt.%, Table 3) generated in the high *T* HyPy step and they exhibit an unusual mature alkane distribution unlike typical Phanerozoic petroleum fluids. A similar carbon number distribution of alkylcyclohexanes (*m/z* 83) and methylalkylcyclohexanes (*m/z* 97) is observed as for *n*-alkanes and supports the likeli-

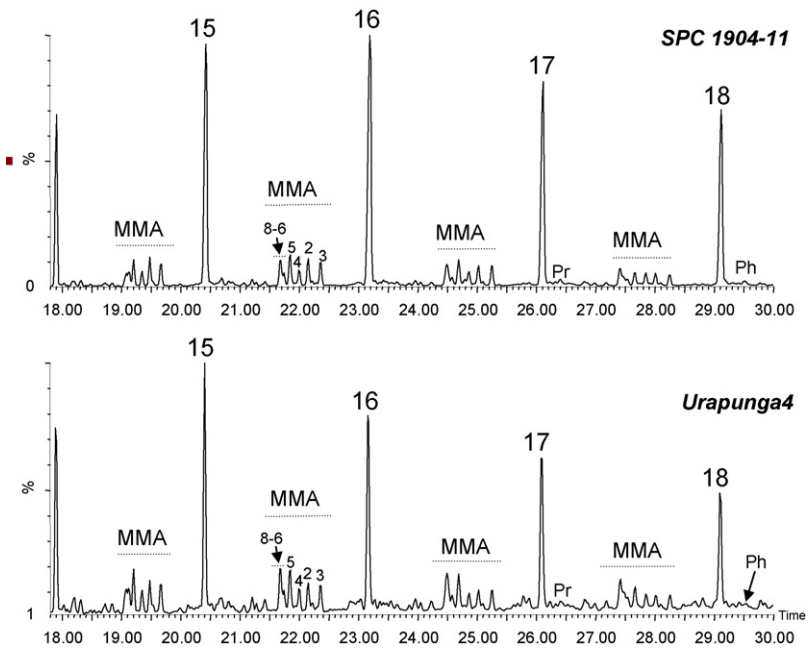


Fig. 15. An expanded view of *m/z* 85 ion chromatograms for SPC 1904-11 and Urapunga4 (Mesoproterozoic) HyPy products, showing the similar distributions of methyl-branched alkanes (MMAs). Numbers associated with MMA clusters (2–8) refer to the position of the methyl-substituent in the linear alkane chain. Other numbers (15–18) refer to the carbon chain length of *n*-alkanes.

hood that the different alkane products generated from a particular kerogen have all undergone the same thermal history.

The mature alkane profile reported here contrasts with the immature alkane pattern reported by Skrzypczak et al. (2006) for another Warrawoona Group kerogen pyrolysate, which shows a distinct even-over-odd carbon number predominance (EOP) in $C_{10}$–$C_{18}$ alkane products, and which is difficult to reconcile with the high thermal maturity and age of typical host Warrawoona kerogens. Thermal cracking is known to remove any biologically inherited carbon number preference of alkyl chains in free and kerogen-bound lipids, even from the earliest stages of catagenesis (e.g., Bowden et al., 2006), and so a distinct EOP of *n*-alkanes is not consistent with these components being genuine Archaean molecular fossils.

In conclusion, PAH units released by HyPy are considerably smaller than the >15 ring aromatic clusters identified by H/C ratios and Raman spectroscopy to comprise, on average, the bulk of the kerogen matrix. These large ring polyaromatic hydrocarbon units are part of the more recalcitrant kerogen portion and are not GC amenable in any case. So, HyPy treatment of Archaean kerogens is only expected to produce a low conversion of kerogen to soluble products although our results do indicate that the compounds generated and detected appear to be informative in any case for assessing thermal maturity and for probing the origins of this highly transformed organic matter. HyPy provides a much more powerful degradation regime than conventional flash pyrolysis (performed in a low pressure inert gas atmosphere, e.g., He) and it is unlikely that these other pyrolysis techniques can generate any significant quantities of bound PAH clusters up to 7 ring aromatic compounds. For example, Skrzypczak et al. (2005) only reported and discussed alkenes and alkylated benzenes up to $C_{30}$ from flash pyrolysis of kerogen from the Apex basalt of the Warrawoona Group.

Future work will concentrate on detailed analysis of any alkanes preserved by trapping in the micropores of the kerogen, but recoverable by HyPy, and whether these contain definitive evidence or otherwise in their molecular and isotopic patterns for a biological origin.

### *4.8. Implications for the origins of kerogen in 3.4–3.5 Ga Warrawoona group cherts*

Obvious similarities (Figs. 10, 14 and 15) exist between both aliphatic and aromatic product profiles obtained from HyPy of Strelley Pool Chert kerogens in comparison with those generated from one middle oil-window-mature Mesoproterozoic kerogen sample (Urapunga4 from 1.45 Ga Velkerri Formation of the Roper Group, Australia). Since this Mesoproterozoic kerogen is biogenic, containing detectable bound hopane and other terpane biomarkers, then the match in molecular profiles offers arguably the most compelling evidence to date for a biogenic origin of Strelley Pool Chert organic matter. Sequential dual temperature experiments on 2 Strelley Pool Chert kerogens suggest that the aromatic hydrocaron products detected were predominantly covalently bound to the kerogen matrix while the alkanes were most likely trapped in the micropores of the kerogen and only released after disruption of the host matrix by some covalent bond cleavage and heating to high temperature. These molecular products are not structurally representative of the large interlinked PAH clusters comprising the average bulk of the organic matter (which are not GC-amenable in any case) and quantitatively comprise less than 2 wt.% of the bulk kerogen. Our investigation has shown though that the extent of alkylation of the aromatic hydrocarbon products generated from the HyPy technique can still sensitively assess the relative thermal maturity ordering of Strelley Pool Chert kerogens. With further study, the molecular and isotope patterns of HyPy products (both trapped/bound alkanes and bound aromatics) offers an attractive opportunity for unraveling the origins of this thermally transformed organic matter.

Ultimately, it is of prime importance to use the spectroscopic, molecular and isotopic results generated to discriminate, if possible, a biogenic from abiogenic mechanism for Archaean kerogen formation. Recently, significant enrichment of $^{12}C$ into organic compounds synthesized abiotically by Fischer Tropsch processes under laboratory simulation of hydrothermal conditions has been reported at one experimental temperature and pressure (McCollom and Seewald, 2006) which can theoretically account for the light stable carbon isotopic signatures of organic matter in the Strelley Pool Cherts. The effect of varying temperature, pressure, the extent of $CO/CO_2$ precursor conversion, and composition of catalytic mineral matrices on the extent of stable carbon fractionation observed have still to be investigated though. It is yet to be demonstrated why the kerogen should be so consistently $^{13}C$-depleted (−28 to −35‰) throughout the vast Strelley Pool Chert unit if an abiotic synthesis pathway is primarily responsible given that temperature, pressure and mineral chemistry fluctuations in the vent system, together with temporal and spatial variations in the extent of reductive conversion of $CO/CO_2$ at the site(s) of organic synthesis, are highly likely.

Furthermore, no detailed molecular mechanism has been proposed to explain how low amounts of simple apolar organics (predominantly low molecular weight *n*-alkanes up to *n*-$C_{32}$ and much lower amounts of analogous *n*-alcohols) produced from Fischer Tropsch synthesis can be transformed into significant quantities of highly aromatic kerogen across wide lateral distances in the Pilbara Craton and neither has this been demonstrated experimentally. It has been assumed that geochemical maturation or metamorphism of almost all naturally occurring organic matter, whether biological or abiological in origin, can ultimately be expected to give rise to essentially the same set of resultant thermally stable products—condensed PAHs bound within a macromolecular matrix. No insoluble organic residue formation was reported, however, from laboratory simulations of hydrothermal organic synthesis at temperature of 250 °C and 325 bar pressure (McCollom and Seewald, 2006) and this remains an unexplained aspect of the abiogenic formation theory. Functionalized lipids (alcohols, fatty acids) can become covalently bound into kerogen when biomass is artificially matured in the laboratory under hydrothermal conditions (Gupta et al., 2004) but this has only been performed in the presence of biopolymers (polysaccharides, proteins, etc.) which degrade and act as reactive nuclei for polymerization. Problems arise when attempting to explain (i) how dissolved apolar organics from hydrothermal fluids can be concentrated up by adsorption or encapsulation in minerals (water being an effective organic solvent at temperatures 200–300 °C) or (ii) how the saturated hydrocarbons and alcohols can be efficiently cross-linked together presumably initially via an aliphatic polymeric matrix which itself is efficiently fragmented under the same hydrothermal conditions (Lewan, 2003).

The most plausible route for forming aromatic-rich kerogen from low molecular weight alkanes and alcohols produced from abiotic Fischer Tropsch synthesis is possibly through pyrobitumen formation, where a recalcitrant residue is left behind after thermal cracking of liquid hydrocarbon constituents at high pressure (ca. 500 bar). This is a poorly understood process, however, and the molecular and isotopic systematics involved in pyrobitumen formation have not been reported to date in any detail in the literature. More work is required to elucidate whether significant quantities of kerogen can be formed from aqueous processing at high *T* (200–300 °C) and high *P* (500 bar) of petroleum condensates and Fischer Tropsch synthesis products, and if so, whether the composition of the insoluble residue is similar to or distinct from Strelley Pool Chert kerogens.

Our preferred explanation at this stage is that the kerogen found in the Strelley Pool Chert was most likely formed from diagenesis and subsequent thermal processing of biogenic organic matter and that the consistent maturity ordering observed in both Raman spectroscopic and HyPy molecular products represents differing degrees of subsequent thermal processing of biogenic kerogen due to the hydrothermal activity and burial regime encountered. While persuasive evidence has been obtained in this investigation which suggests a principally biogenic origin for the insoluble carbonaceous material, such an interpretation is not definitive at this stage. Future work will concentrate on analyzing molecular and isotopic patterns from kerogen hydropyrolysates in detail with GC–MS and GC–IRMS while using Raman spectroscopy to screen and target the less thermally altered black chert zones in the Strelley Pool Chert.

## 5. Conclusions

The combination of elemental analysis, FTIR spectroscopy, Raman spectroscopy, $^{13}C$ NMR spectroscopy, and catalytic hydroprolysis combined with GC–MS analyses shows that kerogen isolated from the ca. 3.43 Ga Strelley Pool Chert, Pilbara Craton, has not reached the graphite stage but consists of a macromolecular network of large polycyclic aromatic units (most probably >15 ring aromatic clusters being most common) containing predominantly short-chain or no aliphatic substituents, covalently cross-linked together. Small amounts of lower molecular weight kerogen-bound polyaromatic constituents (1–7 ring clusters) are still preserved and these can be fragmented by HyPy and analyzed by GC–MS.

Both Raman spectroscopy and detailed molecular analyses of kerogen fragments generated by HyPy have revealed consistent thermal trends within the Strelley Pool Chert sample set. We have showed for the first time a correlation between Raman spectroscopic parameters from intact kerogen, $I_{D1}/I_G$, $I_{D1}/(I_{D1}+I_G)$, and $L_a$ (measurement of structural disorder of macromolecular network and crystallite dimensions) and the extent of alkylation of aromatic hydrocarbons released from HyPy of the kerogen phase. A significant thermal maturity range is apparent (although all samples are overmature with respect to the oil window) governing the bulk chemical structure of kerogen as observed from elemental analysis, Raman spectroscopy and HyPy product analyses. No significant differences in bulk chemical structure between the isolated kerogens from the different black chert samples could be delineated by FTIR spectroscopy and solid-state CP MAS $^{13}C$ NMR spectroscopy but

spectral features are consistent with overmature and highly aromatic kerogen networks.

Obvious similarities are observed between molecular hydrocarbon profiles generated from catalytic hydropyrolysis (HyPy) of 5 Strelley Pool Chert kerogens (3.4 Ga) in comparison with a mature Mesoproterozoic Urapunga4 kerogen (ca. 1.45 Ga) isolated from a marine sediment from the Velkerri Formation of the Roper Group in Northern Territory, Australia, and with the aromatic hydrocarbon profiles reported previously from HyPy of other mature Mesoproterozoic Roper Group kerogens (Brocks et al., 2003) and with overmature late Archaean (ca. 2.5–2.7 Ga) marine kerogens from the Pilbara Craton (Brocks et al., 2003; Eigenbrode, 2004). This is consistent with a biogenic origin for this early Archaean organic matter, although such an interpretation is not definitive at this stage. Further work is required to test whether consistent molecular and compound-specific isotopic patterns can be generated from a larger set of Archaean kerogens, particularly in comparison with any abiogenic kerogen standards that can be produced in the laboratory from aqueous processing under realistic hydrothermal conditions of temperature and pressure.

## Acknowledgments

We are grateful to Dr. Simon George and Dr. Herbert Volk at the Petroleum Organic Geochemistry Group CSIRO for the use of acid digestion facilities. Dr. Elizabeth Carter at the Vibrational Spectroscopy Facility at the University of Sydney is acknowledged for the use of the FTIR and Raman spectrometers and useful discussions. We thank Dr. Alan McCutcheon for NMR analysis at the University of Western Sydney. Alex Bradley (MIT) is acknowledged for help with GC–IRMS analyses. Will Meredith (Nottingham) is thanked for assistance with hydropyrolysis experiments. Jake Waldbauer (MIT) is thanked for helpful comments on an earlier version of the manuscript. C.P.M. would like to thank financial support from the Australian Research Council. A.A. acknowledges an Australian Post-Graduate Award and she and M.R.W. acknowledge the support of Macquarie University including its Biotechnology Research Institute. M.K.V. published with permission of the Director, Geological Survey of Western Australia.

## References

Allwood, A., Walter, M., Marshall, C., Van Kranendonk, M., 2004. Habit and habitat of earliest life on Earth. Abstracts from the Astrobiology Science Conference, NASA, Ames, 28 March–1 April, 2004. Int. J. Astrobiol. 3 (Suppl. 1), 104.

Allwood, A.C., Walter, M.R., Van Kranendonk, M.J., Kamber, B.S., 2005. Life on a transgressive rocky shoreline and carbonate platform: 3.43 Ga Strelley Pool Chert, Pilbara Craton, Western Australia. European Geophysical Union Annual General Meeting Abstract.

Allwood, A.C., Walter, M.R., Kamber, B.S., Marshall, C.P., Burch, I.W., 2006a. Stromatolite reef from the Early Archaean era of Australia. Nature 441, 714–718.

Allwood, A.C., Walter, M.R., Marshall, C.P., 2006b. Raman spectroscopy reveals thermal palaeoenvironments of c.3.5 billion-year-old organic matter. Vib. Spectrosc. 41, 190–197.

Awramik, S.M., Schopf, J.W., Walter, M.R., 1983. Filamentous fossil bacteria from the Archaean of Western Australia. Precambrian Res. 20, 357–374.

Banerjee, N.R., Furnes, H., Muehlenbachs, K., Staudigel, H., de Wit, M., 2006. Preservation of ~3.4–3.5 Ga microbial biomarkers in pillow lavas and hyaloclastites from the Barberton Greenstone Belt, South Africa. EPSL 241, 707–722.

Beny-Bassez, C., Rouzaud, J.N., 1985. Characterisation of carbonaceous materials by correlated electron and optical microscopy and Raman microspectroscopy. Scan. Electron Microsc. 1, 119–132.

Beyssac, O., Rouzaud, J.-N., Goffe, B., Brunet, F., Chopin, C., 2002. Graphitization in a high-pressure, low-temperature metamorphic gradient: A Raman micro-spectroscopy and HRTEM study. Contribut. Mineral. Petrol. 143, 19–31.

Beyssac, O., et al., 2003. On the characterization of disordered and heterogeneous carbonaceous materials by Raman spectroscopy. Spectrochim. Acta Part A 59 (10), 2267.

Bowden, S.A., Farrimond, P., Snape, C.E., Love, G.D., 2006. Compositional differences in biomarker constituents of the hydrocarbon, resin, asphaltene and kerogen fractions: An example from the Jet Rock (Yorkshire, UK). Org. Geochem. 37, 369–383.

Brasier, M.D., Green, O.R., Jephcoat, A.P., Kleppe, A.T., Van Kranendonk, M.J., Lindsay, J.F., Steele, A., Grassineau, N.V., 2002. Questioning the evidence for Earth's oldest fossils. Nature 416, 76–81.

Brasier, M.D., Green, O.R., Lindsay, J.F., McLoughlin, N., Steele, A., Stokes, C., 2005. Critical testing of Earth's oldest putative fossil assemblage from the ~3.5 Ga Apex chert, Chinaman Creek, Western Australia. Precambrian Res. 140, 55–102.

Brocks, J.J., Love, G.D., Snape, C.E., Logan, G.A., Summons, R.E., Buick, R., 2003. Release of bound aromatic hydrocarbons from late Archean and Mesoproterozoic kerogens via hydropyrolysis. Geochim. Cosmochim. Acta 67, 1521–1530.

Bucher, K., Frey, M., 1994. Petrogenesis of Metamorphic Rocks. Springer-Verlag, New York, p. 318.

Buick, R., 1984. Carbonaceous filaments from North Pole, Western Australia: are they fossil bacteria in Archean stromatolites? Precambrian Res. 24, 157–172.

Buick, R., Thornett, J.R., McNaughton, N.J., Smith, J.B., Barley, M.E., Savage, M., 1995. Record of emergent continental crust ~3.5 billion years ago in the Pilbara Craton of Australia. Nature 375, 574–577.

Cuesta, A., Dhamelincourt, P., Laureyns, J., Martinez-Alonso, A., Tascon, J.M.D., 1994. Raman microprobe studies on carbon materials. Carbon 32, 1523–1532.

De Gregorio, B.T., Sharp, T.G., Flynn, G.J., 2005. Compariosn of the structure and bonding of carbon in Apex Chert kerogenous material and Fischer-Tropsch type carbons. Lunar and Planetary Science XXXVI, Abstract #1866.

Derenne, S., Skrzypczak, A., Robert, F., Binet, L., Gourier, D., Rouzaud, J.-N., Clinard, C., 2004. Characterization of the organic

matter in an Archaean Chert (Warrawoona, Australia). Geophys. Res. Abstr. 6, 03612 (EGU06-A-03612).

Dresselhaus, M.S., Dresselhaus, G., 1982. In: Cardona, M., Guntherodt, G. (Eds.), Light Scattering in Solids III. Springer, Berlin, p. 187.

Dunlop, J.S.R., Muir, M.D., Milne, V.A., Groves, D.I., 1978. A new microfossil assemblage from the Archaean of Western Australia. Nature 274, 676–678.

Durand, B., 1980. Kerogen: Insoluble Organic Matter from Sedimentary Rocks. Editions Technip, Paris, p. 519.

Eigenbrode, J.L., 2004. Late Archean microbial ecology: an integration of molecular, isotopic and lithologic studies. Ph.D. Thesis. The Pennsylvania State University (Chapter 4).

Espitalie, J., Laporte, J.L., Madec, M., Marquis, F., Leplat, P., Paulet, J., Boutefeu, A., 1977. Methode rapide de characterization des roches meres, de leur potential petrolier et de leur degree d'evolution. Rev. Inst. Francais Petrole 32, 23–42.

Ferrari, A.C., Robertson, J., 2002. Interpretation of Raman spectra of disordered and amorphous carbon. Phys. Rev. B Condens. Matter Mater. Phys. 61, 14095–14107.

Franz, J., Garcia, R., Love, G.D., Linehan, J., Snape, C.E., 1992. Single pulse excitation $^{13}$C NMR analysis of the Argonne Premium Coals. Energy Fuels 6, 598–602.

Furnes, H., Banerjee, N.R., Muehlenbachs, K., Staudigal, H., de Wit, M., 2004. Early life recorded in Archaean pillow lavas. Science 304, 578–581.

Garcia Ruiz, J.M., Hyde, S.T., Carnerup, A.M., Christy, A.G., Van Kranendonk, M.J., Welham, N.J., 2003. Self-assembled silica-carbonate structures and detection of ancient microfossils. Science 302, 1194–1197.

Gupta, N.S., Briggs, D.E.G., Collinson, M.E., Evershed, R.P., Michels, R., Pancost, R.D., 2004. In situ polymerisation of labile lipids as a source for the aliphatic component of recalcitrant macromolecules in sedimentary materials. Geochim. Cosmochim. Acta 68 (Suppl.), A241.

Hofmann, H.J., Grey, K., Hickman, A.H., Thorpe, R., 1999. Origin of 3.45 Ga coniform stromatolites in Warrawoona Group, Western Australia. Geol. Soc. Am. Bull. 111, 1256–1262.

Hunt, J.M., 1996. Petroleum Geochemistry and Geology, second ed. W.H. Freeman and Company, New York, p. 389.

Jehlicka, J., Urban, O., Pokorny, J., 2003. Raman spectroscopy of carbon and solid bitumens in sedimentary and metamorphic rocks. Spectrochim. Acta A 59, 2341–2352.

Knight, D.S., White, W.B., 1989. Characterization of diamond films by Raman spectroscopy. J. Mater. Res. 4, 385–393.

Komiya, M., Shimoyama, K., 1996. Organic compounds from insoluble organic matter isolated from the Murchison carbonaceous chondrite by heating experiments. Bull. Chem. Soc. Jpn. 69, 53–58.

Kruge, M.A., 2000. Determination of thermal maturity and organic matter type by principal components analysis of the distributions of polycyclic aromatic compounds. Int. J. Coal. Geo. 43, 27–51.

Lepland, A., van Zuilen, M.A., Arrhenius, G., Whitehouse, M.J., Fedo, C.M., 2005. Questioning the evidence for Earth's earliest life—Akilia revisited. Geology 33, 77–79.

Lespade, P., Al-Jishi, R., Dresselhaus, M.S., 1982. Model for Raman scattering from incompletely graphitized carbons. Carbon 5, 427–431.

Lewan, M.D., 2003. Experiments on the role of water in petroleum formation. Geochim. Cosmochim. Acta 61, 3691–3723.

Lindsay, J.F., Brasier, M.D., McLoughlin, N., Green, O.R., Fogel, M., Steele, A., Mertzman, S.A., 2005. The problem of deep carbon and Archean paradox. Precambrian Res. 143, 1–22.

Lowe, D.R., 1980. Stromatolites 3,400-Myr old from the Archaean of Western Australia. Nature 284, 441–443.

Lowe, D.R., 1983. Restricted shallow-water sedimentation of Early Archean stromatolitic and evaporitic strata of the Strelley Pool Chert, Pilbara Block, Western Australia. Precambrian Res. 19, 239–283.

Love, G.D., Snape, C.E., Carr, A.D., Houghton, R.C., 1995. Release of covalently-bound alkane biomarkers in high yields from kerogen via catalytic hydropyrolysis. Org. Geochem. 23, 981–986.

Love, G.D., McAulay, A., Snape, C.E., Bishop, A.N., 1997. Effect of process variables in catalytic hydropyrolysis on the release of covalently-bound aliphatic hyrocarbons from sedimentary organic matter. Energy Fuels 11, 522–531.

Marshall, C.P., Allwood, A.C., Walter, M.R., Van Kranendonk, M.J., Summons, R.E., 2004a. Spectroscopic and microscopic characterization of the carbonaceous material in Archaean Cherts, Pilbara Craton, Western Australia. In: Abstracts of the 21st Annual Meeting of the Society of Organic Petrology: 2004, vol. 21, Sydney, New South Wales, Australia, pp. 107–108.

Marshall, C.P., Allwood, A.C., Walter, M.R., Van Kranendonk, M.J., Summons, R.E., 2004b. Characterization of the carbonaceous material in the 3.4 Ga Strelley Pool Chert, Pilbara Craton, Western Australia. In: Geological Society of America Annual Meeting, Denver, CO, pp. 197–203 (Abstracts with programs).

McCollom, T.M., Seewald, J.S., 2006. Carbon isotope composition of organic compounds produced by abiotic synthesis under hydrothermal conditions. EPSL 243, 74–84.

Meredith, W., Russell, C.A., Cooper, M., Snape, C.E., Love, G.D., Fabbri, D., Vane, C.H., 2004. Trapping hydropyrolysates on silica and their subsequent thermal desorption to facilitate rapid fingerprinting by GC–MS. Org. Geochem. 35, 73–89.

Mojzsis, S.J., Arrhenius, G., McKeegan, K.D., Harrison, T.M., Nutman, A.P., Friend, C.R.L., 1996. Evidence for life on Earth before 3,800 million years ago. Nature 385, 55–59.

Negri, F., Castiglioni, C., Tommasini, M., Zerbi, G., 2002. A computational study of the Raman spectra of large polycyclic aromatic hydrocarbons: Toward molecularly defined subunits of graphite. J. Phys. Chem. A 106, 3306–3317.

Painter, P.C., Snyder, R.W., Starsinic, M., Coleman, M.M., Kuehn, D.W., Davis, A., 1985. Concerning the application of FTIR to the study of coal: A critical assessment of band assignments and the application of spectral analysis programs. Appl. Spectrosc. 35, 475–485.

Pasteris, J.D., Wopencka, B., 2002. Images of Earth's earliest fossils? Nature 420, 476–477.

Pasteris, J.D., Wopencka, B., 2003. Necessary, but not sufficient: Raman identification of disordered carbon as a signature of ancient life. Astrobiology 3, 727–738.

Quirico, E., Rouzaud, J.-N., Bonal, L., Montagnac, G., 2005. Maturation grade of coals as revealed by Raman spectroscopy: Progress and problems. Spectrochim. Acta Part A 61 (10), 2368.

Remusat, L., Derenne, S., Robert, F., Knicker, H., 2005. New pyrolytic and spectroscopic data on Orgueil and Murchison insoluble organic matter: a different origin than soluble? Geochim. Cosmochim. Acta 69, 3919–3932.

Rosing, M.T., 1999. $^{13}$C-depleted carbon microparticles in >3700-Ma sea-floor sedimentary rocks from West Greenland. Science 283, 674–676.

Rouzaud, J.-N., Skrzypczak, A., Bonal, L., Derenne, S., Quirico, E., and Robert, F., 2005. The high resolution transmission electron microscopy: A powerful tool for studying the organization of ter-

restrial and extra-terrestrial carbons. Lunar and Planetary Science XXXVI, Abstract #1322.

Schidlowski, M., 2001. Carbon isotopes as biogeochemical reorders of life over 3.8 Ga of Earth history: evolution of a concept. Precambrian Res. 106, 117–134.

Schopf, J.W., 1993. Microfossils of the Early Arcean apex chert: new evidence of the antiquity of life. Science 260, 640–646.

Schopf, J.W., Kudryavtsev, A.B., Agresti, D.G., Wdowiak, T.J., Czaja, A.D., 2002. Laser-Raman imagery of Earth's earliest fossils. Nature 416, 73–76.

Sephton, M.A., Pillinger, C.T., Gilmour, I., 1999. Small-scale hydrous pyrolysis of macromolecular material in meteorites. Planet. Space Sci. 47, 181–187.

Sephton, M.A., Love, G.D., Watson, J.S., Verchovsky, A.B., Wright, I.P., Snape, C.E., Gilmour, I., 2004. Hydropyrolysis of insoluble carbonaceous matter in the Murchison meteorite: new insights into its macromolecular structure. Geochim. Cosmochim. Acta 68, 1385–1393.

Sephton, M.A., Love, G.D., Meredith, W., Snape, C.E., Sun, C.-G., Watson, J.S., 2005. Hydropyrolysis: a new technique for the analysis of macromolecular material in meteorites. Planet. Space Sci. 53, 1280–1286.

Sharp, T.G., De Gregorio, B.T., 2003. Determining the biogenicity of residual carbon within the Apex Chert. In: The Geological Society of America (GSA), 2003 Seattle Annual Meeting, November 2–5 (Paper No. 187-2).

Skrzypczak, A., Derenne, S., Robert, F., Binet, L., Gourier, D., Rouzaud, J.N., Clinard, C., 2004. Characterization of the organic matter in an Archean chert (Warrawoona, Australia). Geochim. Cosmochim. Acta 68, A240.

Skrzypczak, A., Derenne, S., Binet, L., Gourier, D., Robert, F., 2005. Characterization of a 3.5 Billion year old organic matter: Electron paramagnetic resonance and pyrolysis GC–MS, tools to assess syngeneity and biogenicity. Lunar and Planetary Science XXXVI, Abstract #1351.

Skrzypczak, A., Derenne, S., Robert, F., 2006. Molecular evidence for life in the 3.46 Ba-old Warrawoona chert. Geophys. Res. Abstr. 8, 06203 (EGU06-A-06203).

Stalker, L., Bryce, A.J., Andrew, A.S., 2005. A re-evaluation of the carbon isotopic composition of organic reference materials. Org. Geochem. 36, 827–834.

Tuinstra, F., Koenig, J.L., 1970. Raman spectra of graphite. J. Chem. Phys. 53, 1126–1130.

Ueno, Y., Isozaki, Y., Yurimoto, H., Maruyama, S., 2001a. Carbon isotopic signatures of individual Archaean microfossils (?) from Western Australia. Int. Geol. Rev. 43, 196–212.

Ueno, Y., Isozaki, Y., Yurimoto, H., Maruyama, S., 2001b. Early Archean (ca. 3.5) microfossils and 13C-depleted carbonaceous matter in the North Pole area, Western Australia. Field occurrence and geochemistry. In: Nakashima, S., Maruyama, S., Brack, A., Windley, B.F. (Eds.), Geochemistry and the Origin of Life. Universal Academy Press, pp. 203–236.

Ueno, Y., Yurimoto, H., Yoshioka, H., Komiya, T., Maruyama, S., 2002. Ion microprobe analysis of graphite from ca. 3.8 Ga meta-sediments, Isua supracrustal belt, West Greenland: Relationship between metamorphism and carbon isotopic composition. Geochim. Cosmochim. Acta 45, 1257–1268.

Ueno, Y., Yoshioka, H., Maruyama, S., Isozaki, Y., 2004. Carbon isotopes and petrography of kerogens in ~3.5 Ga hydrothermal silica dikes in the North Pole area, Western Australia. Geochim. Cosmochim. Acta 68, 573–589.

Van Kranendonk, M.J., 2000. Geology of the North Shaw 1:100 000 sheet: Western Australia Geological Survey, 1:100 000. Geological Series Explanatory Notes, 86 pp.

Van Kranendonk, M.J., Pirajno, F., 2004. Geological setting and geochemistry of metabasalts and alteration zones associated with hydrothermal chert ± barite deposits in the ca. 3.45 Ga Warrawoona Group, Pilbara Craton, Australia. Geochem. Explor. Environ. Anal. 4, 253–278.

Van Kranendonk, M.J., Hickman, A.H., Smithies, R.H., Nelson, D.N., Pike, G., 2002. Geology and tectonic evolution of the Archaean North Pilbara terrain, Pilbara Craton, Western Australia. Econ. Geol. 97, 695–732.

Van Kranendonk, M.J., Webb, G.E., Kamber, B.S., 2003. Geological and trace element evidence for a marine sedimentary environment of deposition and biogenicity of 3.45 Ga stromatolitic carbonates in the Pilbara Craton, and support for a reducing Archaean ocean. Geobiology 1, 91–108.

Van Kranendonk, M.J., Smithies, R.H., Hickman, A.H., Bagas, L., Williams, I.R., Farrell, T.R., 2005. Event stratigraphy applied to 700 m.y. of Archaean crustal evolution, Pilbara Craton, Western Australia. Western Australia Geological Survey. Annu. Rev. 2003–2004, 49–61.

Walter, M.R., Buick, R., Dunlop, J.S.R., 1980. Stromatolites, 3,400–3,500 Myr old from the North Pole area, Western Australia. Nature 284, 443–445.

Westall, F., Rouzaud, J.N., 2004. Carbonaceous microfossils in Early Archean cherts. Geochim. Cosmochim. Acta 68, A239.

Wopenka, B., Pasteris, J.D., 1993. Structural characterization of kerogens to granulite-facies graphite: applicability of Raman microprobe spectroscopy. Am. Miner. 78, 533–557.

Yui, T.-F., Huang, E., Xu, J., 1996. Raman spectrum of carbonaceous material: A possible metamorphic grade indicator for low-grade metamorphic rocks. J. Metamorphic Geol. 14, 115–124.